Title

Metabolic Syndrome Mediates ROS-miR-193b-NFYA–Dependent Downregulation of Soluble Guanylate Cyclase and Contributes to Exercise-Induced Pulmonary Hypertension in Heart Failure With Preserved Ejection Fraction

Journal

Circulation, 144(8)

ISSN

0009-7322

Authors

Satoh, Taijyu
Wang, Longfei
Espinosa-Diez, Cristina
et al.

Publication Date

2021-08-24

DOI

10.1161/circulationaha.121.053889

Peer reviewed

Published in final edited form as:

Circulation. 2021 August 24; 144(8): 615–637. doi:10.1161/CIRCULATIONAHA.121.053889.

Metabolic syndrome mediates ROS-miR-193b-NFYA-dependent down regulation of sGC and contributes to exercise-induced pulmonary hypertension in HFpEF

Taijyu Satoh, MD, PhD[1], **Longfei Wang, MD**[1], **Cristina Espinosa-Diez, PhD**[1], **Bing Wang, MD, PhD**[2], **Scott A. Hahn, MS**[1], **Kentaro Noda, PhD**[3], **Elizabeth R. Rochon, PhD**[1], **Matthew R. Dent, PhD**[1], **Andrea Levine, MD**[4], **Jeffrey J. Baust, BS**[1], **Samuel Wyman, BS**[5], **Yijen L. Wu, PhD**[5], **Georgios A. Triantafyllou, MD**[6], **Ying Tang, MS**[1,7], **Mike Reynolds, BS**[1], **Sruti Shiva, PhD**[1,8], **Cynthia St Hilaire, PhD**[1,7,9], **Delphine Gomez, PhD**[1,7], **Dmitry A. Goncharov, BS**[1,10], **Elena A. Goncharova, PhD**[1,9,10], **Stephen Y. Chan, MD, PhD**[1,7], **Adam C. Straub, PhD**[1,8], **Yen-Chun Lai, PhD**[11], **Charles F. McTiernan, PhD**[1], **Mark T. Gladwin, MD**[1,6]

[1]Pittsburgh Heart, Lung and Blood Vascular Medicine Institute, University of Pittsburgh School of Medicine, Pittsburgh, PA, USA.

[2]Departments of Orthopedic Surgery, University of Pittsburgh, Pittsburgh, PA, USA

[3]Division of Lung Transplant and Lung Failure, Department of Cardiothoracic Surgery, University of Pittsburgh, Pittsburgh, PA, USA

[4]Pulmonary & Critical Care Medicine, University of Maryland School of Medicine, Baltimore, MD, USA

[5]Rangos Research Center Animal Imaging Core and Developmental Biology, University of Pittsburgh, Pittsburgh, PA, USA

[6]Division of Pulmonary, Allergy and Critical Care Medicine, University of Pittsburgh School of Medicine, Pittsburgh, PA, USA.

[7]Division of Cardiology, University of Pittsburgh School of Medicine, Pittsburgh, PA, USA

[8]Department of Pharmacology and Chemical Biology, University of Pittsburgh School of Medicine, Pittsburgh, PA, USA

[9]Department of Bioengineering, University of Pittsburgh School of Medicine, Pittsburgh, PA, USA

[10]Division of Pulmonary, Critical Care and Sleep Medicine, University of California Davis, Davis, CA, USA

[11]Division of Pulmonary, Critical Care, Sleep and Occupational Medicine, Indiana University School of Medicine, Indianapolis, IN, USA.

Abstract

Address for Correspondence: Mark T. Gladwin, MD, Pittsburgh Heart, Lung, Blood, and Vascular Medicine Institute, University of Pittsburgh, Pittsburgh, PA 15261; gladwinmt@upmc.edu.

Background: Many patients with heart failure with preserved ejection fraction (HFpEF) have metabolic syndrome and develop exercise-induced pulmonary hypertension (EIPH). Increases in pulmonary vascular resistance in patients with HFpEF portend a poor prognosis; this phenotype is referred to as combined pre-and post-capillary PH (CpcPH). Therapeutic trials for EIPH and CpcPH have been disappointing, suggesting the need for strategies that target upstream mechanisms of disease. This work reports novel rat EIPH models and mechanisms of pulmonary vascular dysfunction centered around the transcriptional repression of the soluble guanylate cyclase (sGC) enzyme in pulmonary artery smooth muscle cells (PAVSMCs).

Methods: We used obese ZSF-1 leptin-receptor knock-out rats (HFpEF model), obese ZSF-1 rats treated with SU5416 to stimulate resting PH (Obese+sugen, CpcPH model), and Lean ZSF-1 rats (controls). Right and left ventricular hemodynamics were evaluated via implanted-catheters during treadmill exercise. PA function was evaluated using MRI and myography. Overexpression of NFYA, a transcriptional-enhancer of sGCβ1, was performed by PA delivery of adeno-associated-virus 6 (AAV6). Treatment groups received SGLT2 inhibitor Empagliflozin in drinking water. PAVSMCs from rats and humans were cultured with Palmitic acid, Glucose, and Insulin (PGI) to induce metabolic-stress.

Results: Obese rats showed normal resting right ventricular systolic pressures (RVSP) which significantly increased during exercise, modeling EIPH. Obese+sugen rats showed anatomical PA remodeling and developed elevated RVSP at rest, which was exacerbated with exercise, modeling CpcPH. Myography and MRI during dobutamine-challenge revealed PA functional impairment of both obese groups. PAs of obese rats produced reactive oxygen species (ROS) and decreased sGCβ1 expression. Mechanistically, cultured PAVSMCs from obese rats, humans with diabetes or treated with PGI, showed increased mitochondrial-ROS, which enhanced miR-193b-dependent RNA-degradation of NFYA, resulting in decreased sGCβ1-cGMP signaling. Forced NYFA expression by AAV6 delivery increased sGCβ1 levels and improved exercise-PH in Obese+sugen rats. Treatment of Obese+sugen rats with Empagliflozin improved metabolic syndrome, reduced mitochondrial ROS and miR-193b levels, restored NFYA/sGC activity, and prevented EIPH.

Conclusions: In HFpEF and CpcPH models, metabolic syndrome contributes to pulmonary vascular dysfunction and EIPH through enhanced ROS and miR-193b expression, which down-regulates NFYA-dependent sGCβ1 expression. AAV-mediated NFYA overexpression and SGLT2 inhibition restores NFYA-sGCβ1-cGMP signaling and ameliorates EIPH.

Keywords

EIPH; CpcPH; NFYA; miR-193b; nitric oxide

Introduction

Heart failure has been estimated to afflict nearly 26 million people worldwide, with more than 50% of patients having heart failure with preserved ejection fraction (HFpEF).[1–3] HFpEF is defined by clinical features of heart failure, with an ejection fraction (EF) greater than 50% and imaging evidence of left ventricular diastolic dysfunction.[4] The burgeoning epidemic of HFpEF is largely related to the concomitant increased prevalence of diabetes,

hypertension, hyperlipidemia, obesity, and increasing age of our population, all known risk factors for HFpEF.[5]

Pulmonary hypertension is a common complication of HFpEF which is associated with high morbidity and mortality. The World Health Organization classifies pulmonary hypertension due to left heart disease as Group 2 pulmonary hypertension which incorporates HFpEF, HFrEF, as well as valvular disease.[6] Despite being the most common form of pulmonary hypertension, there are no approved therapies for the treatment of pulmonary hypertension secondary to HFpEF.[6] By right heart catheterization, pulmonary hypertension due to left heart disease is defined by a mean pulmonary artery pressure (mPAP) ≥ 25 mmHg (new definitions even consider values ≥ 20 mmHg) and a pulmonary artery occlusion pressure (PAOP) > 15 mmHg.[7] Two major mechanisms have been considered central to the development of high pulmonary pressures. 1) passive hypertension with chronic passive increases in left ventricular end-diastolic pressure (LVEDP); 2) vascular dysfunction and cellular remodeling, with chronic increases in pulmonary pressures compounded by dysregulated vaso-motor signaling pathways driven by the associated metabolic syndrome (insulin resistance, obesity, hypertension). Both processes lead to high right ventricular afterload and failure.

A major symptom of HFpEF is exertional dyspnea and exercise intolerance, in large part related to significant increases in pulmonary pressures during exercise, referred to as exercise induced pulmonary hypertension (EIPH).[8,9] EIPH may represent an early stage of pulmonary hypertension, and portends an overall worse prognosis, with higher risk of right ventricular dysfunction and death.[10,11] Recently, clinical data have been proposed to define diagnostic criteria for EIPH.[12] A European Respiratory Society Task Force has recommended the diagnosis of EIPH as mean pulmonary artery pressure (mPAP) >30 mmHg and total pulmonary resistance (TPR) >3 Wood units at peak exercise.[13] Importantly, more than half of patients with HFpEF develop EIPH,[9] although the mechanism linking HFpEF and EIPH remains unclear.

Patients with HFpEF who develop an increase in pulmonary artery pressures at rest that are substantially higher than the left ventricular diastolic pressure are now referred to as combined pre-and post-capillary pulmonary hypertension (CpcPH).[14,15] The hemodynamic criteria for CpcPH has been defined by a high transpulmonary pressure gradient, diastolic pressure gradient or pulmonary vascular resistance, all of which are associated with higher risk of death than having HFpEF without intrinsic pulmonary vascular disease.[16–18] In the setting of HFpEF, EIPH and CpcPH likely represent advancing spectrums of the severity of pulmonary vascular dieases, with EIPH representing an earlier manifestation where the resting pressures may be normal but rise pathologically during exercise, while patients with CpcPH have resting high pulmonary vascular resistance and severe exercise PH with RV dysfunction.[17] Despite a clear understanding of the clinical risk related to both EIPH and CpcPH in the setting of HFpEF, the underlying mechanisms that drive pulmonary vascular functional impairment remain unknown, in large part related to the lack of relevant pre-clinical models of disease.[19]

A central risk factor for the development of CpcPH in the setting of HFpEF is the metabolic syndrome. In fact, more than 80% of patients with HFpEF have one or more feature of the metabolic syndrome. In a mouse model, combination of inhibition of NO synthases and metabolic syndrome (high fat diet) induces a cardiac phenotype consistent with HFpEF.[20] Similarly, rats with leptin receptor knock-out (ZSF-1) develop features of metabolic syndrome and develop HFpEF. In order to develop a model of CpcPH, we exposed ZSF-1 obese rats to the VEGF inhibitor Sugen (100mg/kg SU5416) to trigger pulmonary vascular remodeling.[21] In the current study we explore the effects of acute exercise stress on both the ZSF-1 obese rat without Sugen treatment, which has HFpEF without baseline pulmonary hypertension, and with Sugen treatment, which has CpcPH at rest. The former models EIPH with significant pulmonary hypertension developing with exercise, while the later model CpcPH develops even more severe PH and right ventricular dysfunction with exercise.

In the current study we report that these rat models of EIPH and CpcPH develop intrinsic pulmonary vascular disease with impaired vasodilatory capacity during exercise. An examination of isolated pulmonary vasculature and pulmonary artery vascular smooth muscle cells (PAVSMCs) reveals a significant impairment in the nitric oxide (NO) signaling pathway, which unexpectedly is caused by a profound depletion in the enzyme soluble guanylate cyclase (sGC), such that even in the presence of adequate endogenous or therapeutic NO the enzyme cannot be activated to produce vasodilatory cGMP. NO is normally produced by endothelium-dependent NO synthase (eNOS) and diffuses to smooth muscle and activates its specific receptor soluble guanylyl cyclase (sGC), which in turn converts 3’−5’ guanosine triphosphate (GTP) to cyclic 3’−5’ guanosine monophosphate (cGMP), which promotes smooth muscle relaxation and vasodilation.[22] Impaired NO-sGC-cGMP signaling has been described in patients with diabetes, mediated by the activation of oxidases which produce superoxide and reduce the expression or activity of eNOS.[23] In disease states like diabetes, increased vascular ROS may directly oxidize the heme moiety of sGC which inhibits NO binding and causes heme loss, which leads to sGC ubiquitination and degradation.[24] However, in the studies presented here we find that high levels of vascular ROS dramatically reduce the transcription of sGC, rather than scavenge NO or oxidize and proteolyze the enzyme.

The transcriptional regulation of sGCβ1 expression is incompletely understood in the PAVSMCs or in the setting of HFpEF, although multiple proteins including several FoxOs, growth factor independence 1, and Nuclear factor Y alpha (NFYA) have been reported as transcription factors regulating sGC expression in other cell types and diseases.[25,26] As a component of the NFY complex, NFYA is one of the most robust transcription factors binding to CCAAT- boxes, of which three are found in the sGCβ1 promoter region.[27] As a regulator of smooth muscle cell proliferation and hepatocyte gluconeogenesis, NFYA may have an important role in vascular diseases related to metabolic syndrome.[28,29] The data presented here suggest that this is mediated by production of mitochondrial ROS that in turn reduces the levels of the transcription factor NFYA, which in PAVSMC is required for sGCβ1 expression.

Due to their regulation of mRNA turnover and translation, microRNAs have been shown to play an important role in the pathophysiology (e.g. cellular proliferation, vasoconstriction, inflammation, metabolism) of pulmonary hypertension.[30,31] miR-193b promotes NFYA transcript degradation in white adipose tissue and is increased in diabetic humans.[32,33] In the current study we evaluate the central role of NFYA in the transcriptional control of sGCβ1 expression in the pulmonary vasculature and upstream processes regulating NFYA expression via miR-193b. Whereas increased ROS generation and impaired NO and cGMP signaling have been implicated in the metabolic syndrome,[34,35] and most patients with HFpEF exhibit features of the metabolic syndrome, the transcriptional dysregulation of sGCβ1 expression and important role of NFYA in EIPH and CpcPH in the setting of HFpEF have not been previously characterized. Leveraging the current findings of metabolic syndrome-ROS-NFYA-sGCβ1 signaling, we demonstrate that therapeutic forced expression of NFYA using AAV6 intravascular gene delivery restores sGCβ1 expression and cGMP signaling and improves EIPH and CpcPH.

Therapies that directly target the pulmonary vasculature or left ventricle in the setting of HFpEF have to date been disappointing[19,36], suggesting the need for strategies that target upstream disease mechanisms, such as metabolic syndrome and impaired vascular redox homeostasis (high ROS formation/impaired nitric oxide-soluble guanylate cyclase-cGMP signaling). Here we have developed a novel rat EIPH model with metabolic syndrome, and therapeutically target upstream metabolic syndrome and secondary vascular reactive oxygen species (ROS) formation using a SGLT2 inhibitor. SGLT2 inhibitor therapy is associated with decreases in heart failure related hospitalization, non-fatal myocardial infarction and cardiovascular death in adult patients with type 2 diabetes and cardio-vascular risk.[37,38] SGLT2 inhibitors improve cardiovascular risk factors through lower blood glucose levels, lower blood pressure via osmotic diuresis, and increased urinary caloric loss with reductions in body weight. However, it remains unclear why SGLT2 inhibitors show superior outcomes relative to other diabetes therapeutics (such as metformin) or diuretic drugs, despite a lack of SGLT2 expression in the myocardium or any vasculature other than in the kidney. Considering the high prevalence of metabolic syndrome features in patients with HFpEF, and prior findings of strong relation between metabolic dysfunction and exercise intolerance[39], the inhibition of SGLT2 may represent an effective upstream treatment strategy for both EIPH and CpcPH in the setting of HFpEF.

Materials and Methods

METHODS

The data that support the findings of this study are available from the corresponding author upon reasonable request. Detailed methods and materials are available in the online Data Supplement. Methods include surgical catheter placement and assessment of hemodynamics during rat treadmill testing, ultrasonography, cardiac MR imaging in response to dobutamine challenge, myography, measurement of rat plasma factors (e.g., cGMP), microscopic analyses, tissue culture of rat and human pulmonary artery (PA) vascular smooth muscle cells (PAVSMCs) in standard and metabolic-syndrome-inducing media (PGI), mitochondrial complex activity, RNA and protein isolation and analysis.

Animal and Human Subjects and Ethical Considerations—All animal procedures were reviewed and approved by the University of Pittsburgh Institutional Animal Care and Use Committee. De-identified early-passage (3–8) human PAVSMCs were provided by the University of Pittsburgh Cell Processing Core. De-identified lung tissue specimens for cell isolation were obtained from the University of Pittsburgh Tissue Medical Center Transplant program and Tissue Donation Program at the University of Pittsburgh Medical Center, under the protocols approved by the University of Pittsburgh IRB and CORID. Human and rat PAVSMC isolation, maintenance, and characterization were performed as previously described.[40]

Statistical Analyses—All results are shown as mean ± SEM. Normality of data was confirmed by Shapiro Wilk testing (JMP 15 software, SAS Institute, North Carolina, USA), which revealed normal distribution of all data. An F-test was used to test the equality of variance in two independent groups. Comparisons of means between 2 groups with equal variances were performed by 2-tailed Student's *t*-test, while 2 groups with unequal variances were compared by Welch's t-test. Comparisons of mean responses associated with the two main effects of the different genotypes was performed by two-way analysis of variance (ANOVA) with interaction testing, followed by Tukey's HSD (honestly significant difference) for multiple comparisons. When comparing more than two groups, the data were analyzed using one-way ANOVA, followed by Tukey's HSD as all data showed normal distribution. When comparing hemodynamic and other parameters between different groups of rats at rest and during exercise, data were analyzed using repeated measures two-way ANOVA (if the number of rats in each group was the same) or mixed-effects model analysis (if the number of rats in each group rat was different) as the data was taken over time from the same rat. Fasting Glucose and GTT data were also analyzed by two-way repeated measures ANOVA or mixed-effects model analysis. Statistical significance was evaluated with GraphPad Prism 7 (GraphPad Software, San Diego, USA). All reported P values are 2-tailed, with a P value of less than 0.05 considered statistically significant.

Results

Development of a rat model of exercise-induced pulmonary hypertension (EIPH) with HFpEF

We and others have previously reported that the ZSF-1 obese rat displays metabolic syndrome and pathophysiologic features consistent with HFpEF[21,41], and that these animals develop resting pulmonary hypertension after additional treatment with the vascular endothelial growth factor receptor-2 antagonist SU5416 (obese+sugen), modeling human CpcPH.[21] Here, we tested the effects of exercise on cardiopulmonary hemodynamics in the HFpEF (Obese) and CpcPH (obese+sugen) model rats, and compared to lean (non-obese) treated with or without SU5416 (lean+sugen) as controls. At 8 weeks of age, lean and obese rats were treated with Sugen (100mg/kg) (Figure 1A). At 20 weeks of age, all rats (lean, lean+sugen, obese, and obese+sugen rats) were implanted with 3 Fr polyethylene tubes into the right (RV) and left ventricles (LV) (Figure 1B and Figure I-A–B in the Supplement). After 1 week of familiarization and training with the treadmill, a stepwise treadmill exercise protocol was performed to determine the maximal treadmill speed for each rat (Figure I-C in

the Supplement), during which their workload was also measured. Two days later, RV and LV pressures were measured during exercise at maximal speed for 30 minutes (Figure 1A and Figure I-D in the Supplement).

Obese rats and obese+sugen rats developed metabolic syndrome (elevated body weight, HbA1c, triglyceride, insulin, abnormal glucose tolerance test, and insulin resistance measured as the homeostatic model assessment for insulin resistance (HOMA-iR) (Figure 1C–D and Figure I-F–G in the Supplement). At rest, obese rats showed normal RVSP, higher left ventricular end-diastolic pressure (LVEDP) and modest elevations in mean pulmonary arterial pressure (mPAP) compared to lean and lean+sugen rats (Figure 1E, Figure I-H and Table I in the Supplement). Obese+sugen rats developed elevated RVSP and mPAP at rest compared with lean, lean+sugen and obese rats (Figure 1E and Figure I-H in the Supplement). During exercise, both obese rats and obese+sugen rats showed significantly increased RVSP and RVEDP when compared to either lean-exercised or their corresponding resting hemodynamic values (Figure 1E). Lean+sugen rats slightly increased exercise-induced increase in RVSP compared to lean rats, but this was not significant (Figure 1E). During exercise, lean and obese group rats showed a similar and significant increase in LVEDP, systolic BP (LVSP), heart rate and respiratory rate (Figure 1E and Figure I-I in the Supplement). To normalize the effect of body weight on workload, each workload was multiplied by bodyweight as previously described.[42] Obese and obese+sugen rats showed a significantly decreased “workload x bodyweight”, suggesting poor exercise tolerance (Figure 1F). Obese+sugen rats also developed a higher Fulton index compared with lean, lean+sugen and obese rats, indicating right ventricular hypertrophy (Figure 1G and Figure I-J in the Supplement). These results suggest that obese rats without sugen treatment displayed cardiac function measures consistent with EIPH (EIPH model), whereas obese+sugen rats had resting and more severe exercise-exacerbated PH and cardiac dysfunction, validating a model of CpcPH with more severe EIPH.

Right ventricular dysfunction after exercise in HFpEF model rats

Doppler-ultrasonography was performed to evaluate cardiac function at rest and after exercise. At rest, ZSF-1 obese rats showed cardiac dysfunction consistent with HFpEF, with preserved ejection fraction and lower E/A ratio relative to lean rats, consistent with prior publications (Figure 2A–B and Table II in the Supplement).[41] Post exercise, lean and lean+sugen rats significantly increased cardiac output (CO) and cardiac index (CI), which failed to increase in obese and obese+sugen rats (Figure 2C). Obese+sugen rats, but not obese rats, developed RV dysfunction even at rest, as assessed by significantly increased RVDd and numerically decreased PAAT/ET ratios (Figure 2D and E). After exercise, obese rats also developed right ventricular dysfunction (significantly increased RVDd and decreased PAAT/ET ratio and TAPSE (Figure 2E). After exercise, obese+sugen rats demonstrated a significant decrease in RV function parameters (Figure 2E). From the RVSP and cardiac index values, the calculated total pulmonary resistance index (TPRi) was increased in obese+sugen rats at rest. After exercise, both obese and obese+sugen rats showed higher TPRi compared to either lean- and lean+sugen-exercised or their corresponding resting hemodynamics (Figure 2F). Strain ultrasonography was used to evaluate early or subtle changes in RV and LV function. At rest, LV circumferential and

longitudinal strain were lower in obese and obese+sugen rats when compared to lean rats, resembling human HFpEF patients (Table III in the Supplement). After exercise, RV longitudinal strain was decreased in obese rats (Table III in the Supplement). These data show that obese HFpEF rats develop RV dysfunction after exercise, consistent with the criteria for EIPH. Similarly, obese+sugen rats also showed numerically worse RV dysfunction after exercise, suggesting poor cardiac function during exercise in CpcPH. These results suggest that EIPH and CpcPH model rats increase pulmonary artery resistance during exercise, compounding exercise induced increases in LVEDP, which increases right ventricle pressures, impairs RV function, and worsens exercise capacity, similar to observations in humans with HFpEF who develop EIPH and CpcPH.[8,11]

Physiological mechanisms of pulmonary hypertension with exercise in HFpEF model rats

Immunohistochemical analysis with αSMA staining showed modest but significant remodeling, with increases in PA medial thickness in obese+sugen rats compared with lean and obese rats (Figure 3A). Lean+sugen rats showed slightly higher PA medial index compared to lean rats, but this was more substantial in the obese+sugen rats, as previously reported.[21] In patients with PAH, MR imaging demonstrates dilation of PAs and decreased vasoconstriction, which reflect severity of PH.[43] We therefore evaluated PA size and vasodilatation using MRI in our EIPH and CpcPH models, during dobutamine infusions to model exercise stress and prevent motion interference during lung imaging. Dobutamine increases CO and heart rate without increasing LV pressure or peripheral arterial vasoconstriction, ideally testing pulmonary vascular responses to increasing flow without increasing LVEDP.[44] Dobutamine infusions also allow for *in vivo* imaging of the lung vasculature responses to high cardiac output which are not technically possible in conscious exercising rats. At rest, MR imaging showed dilated PA and RV in the obese+sugen rats compared with lean, lean+sugen and obese rats, consistent with chronically elevated pulmonary pressures and PA dilatation (Figure 3B and Figure II-A in the Supplement). During dobutamine challenge, lean and lean+sugen rats exhibited PA dilation as cardiac output increased; in contrast obese rats and obese+sugen rats failed to dilate their pulmonary arteries and increased RV dilation (Figure 3B). We note that the use of anesthesia (isoflurane 2%) during MRI decreased the difference in resting RV and LV systolic pressure among all rats compared to the difference in resting hemodynamics without anesthesia in Figure 1E. However, CpcPH rats still showed higher resting RVSP compared to lean rats during MRI (Figure 3C). With dobutamine challenge, lean rats did not increase RV and LV pressures, whereas obese and obese+sugen rats significantly increased RVSP and RVEDP without a significant increase in LVSP and LVEDP when compared to either lean- and lean+sugen-dobutamine or their corresponding resting hemodynamics (Figure 3C and Table IV in the Supplement). Ultrasonography during dobutamine challenge revealed an increase in CO in lean, lean+sugen and obese rats, which was not seen in obese+sugen rats (Figure 3C and Figure II-B and Table V in the Supplement). Both obese rats and obese+sugen rats increased RV dilation and decreased PAAT/ET time, suggesting dobutamine-induced RV dysfunction (Figure II-B in the Supplement). In aggregate, these studies reveal functional pulmonary vascular impairment during dobutamine infusions in both ZSF-1 rats with and without sugen, independent of changes in LVEDP. While the CpcPH model is more severe with resting PH and evident pulmonary artery smooth muscle

hypertrophy and proliferation, the milder EIPH model does develop pulmonary vascular dysfunction that becomes evident by ultrasonographic and MR imaging during both exercise or dobutamine infusions. Considering these data, we propose that the EIPH model ZSF-1 rats exhibit functional pulmonary arterial impairments even without pathologically evident pulmonary arterial remodeling that is seen in the CpcPH model rats (Figure 3E and Figure II-B in the Supplement).

Increased mitochondrial derived ROS and decreased sGC enzyme expression and activity in PAVSMCs

To further explore the mechanisms of pulmonary vascular dysfunction, *ex vivo* vessel myography studies on isolated pulmonary arteries of obese ZSF-1 rats were performed. Pulmonary arteries of both obese rats showed impaired vasodilation responses to acetylcholine (Ach) and sodium nitroprusside (SNP, NO donor), suggesting functional impairments in endothelial-dependent and independent function, even in the absence of structural pulmonary vascular smooth muscle remodeling (Figure 4A). As increased oxidative stress is a major pathophysiologic consequence of metabolic syndrome[35] and modulates vascular relaxation via down-regulation of eNOS or cGMP production from soluble guanylate cyclase (sGC)[45], oxidative stress biomarkers were measured in lean, obese, and obese+sugen rats. Immunofluorescence staining demonstrated high levels of 4-hydroxynonenal (4HNE) and 8 hydroxy-2 deoxy guanosine (8-OHdG), used to assess ROS-mediated lipid peroxidation and DNA oxidation, respectively, around the pulmonary arteries of obese and obese+sugen rats at rest and after exercise (Figure 4B and Figure III-A in the Supplement). Oxidized LDL plasma levels were also higher in obese and obese+sugen rats compared to lean, and further increased after exercise, consistent with a significant increase in ROS in these animals (Figure III-B in the Supplement). Considering the abnormal pulmonary artery function in obese rats, primary cultures of PAVSMCs were isolated from 6 different obese and lean rats and used to characterize ROS production. Cells were characterized by predominant positive staining with smooth muscle specific antibodies (αSMA and SM22), and sparse to absent staining with von Willebrand Factor (vWF) to distinguish from endothelial cells (Figure III-C in the Supplement). Intra-cellular ROS (CellROX positive/negative cell ratio), mitochondrial ROS (MitoSOX positive/negative cell ratio), and membrane potential (TMRM strong/weak positive cell ratio) were all significantly increased in cultured PAVSMCs of obese compared to lean rat PAVSMCs (Figure 4C–D). The intra-cellular ROS in obese PAVSMCs were normalized by treatment with MitoTEMPO (50μM, 10 min) and largely decreased by treatment with Rotenone (10μM, 10 min), indicating that the ROS is primarily derived from mitochondria (Figure 4C), although incomplete quenching of ROS suggests additional oxidase sources. Relative to appropriate controls, mitochondrial complex activity and UCP2 expression were higher in PAVSMCs from obese rats (complex I, II, III, IV), whereas ATP levels were unaltered (Figure III-D–E in the Supplement).

As key regulators of cardiopulmonary function, plasma levels of cGMP, cAMP, PDE5, ANP, and BNP were measured at rest and after 30 minutes of exercise. Whereas lean rats increased plasma cGMP levels after exercise for 30 minutes, both obese and obese+sugen had significantly lower cGMP levels at rest that did not increase after exercise (Figure

4E). On the other hand, cAMP, PDE5, ANP and BNP plasma levels were similar amongst all groups (Figure III-F in the Supplement). In addition, western blotting and RT-PCR of isolated left main pulmonary artery homogenate from obese rats revealed significantly lower sGCβ1 protein and mRNA levels, with a trend towards a further decrease in obese+sugen rats (Figure 4F and Figure III-G in the Supplement). sGCβ1 expression was not significantly different between lean and lean+sugen rats (Figure III-H in the Supplement). Similarly, sGCα1 expression was numerically, but not significantly, decreased in pulmonary arteries of obese rats, while pulmonary arteries of obese+sugen rats showed significant decrease in sGCα1 expression (Figure 4F and Figure III-G in the Supplement). RT-PCR and western blotting demonstrated eNOS mRNA and phosphorylation were not significantly different between pulmonary arteries of lean and obese rats while obese+sugen rats showed a significant decrease compared to lean rats (Figure 4F and Figure III-G in the Supplement). Additionally, PDE5 expression in pulmonary arteries were not altered in protein and mRNA level among lean, obese and obese+sugen rats (Figure III-I–J in the Supplement). Moreover, immunofluorescence staining demonstrated lower expression of sGCβ1 in the pulmonary arteries of obese and obese+sugen rats at rest, which were further decreased after exercise (Figure 4G).

Consistent with reduced sGCβ1 enzyme levels, obese and obese+sugen PAVSMCs showed less cGMP formation with NO donor treatment (10 μM NONOate) (Figure 4H). Moreover, obese PAVSMCs showed poor response to sGC activator (BAY 60–2770) and stimulators (BAY 41–8543) compared to lean ZSF-1 PAVSMCs (Figure III-K in the Supplement). In order to assess NO-sGC responsiveness, obese and lean rats were treated with sodium nitrite (NO_2^-), which is metabolized *in vivo* to form NO, via drinking water (100 mg/L) for 1-week. The nitrite treatment did not increase cGMP plasma levels and sGCβ1 expression in obese rats while lean rats showed significant increase in cGMP plasma level (Figure 4I and Figure IV-A in the Supplement). Consistent with a lack of effect of nitrite on sGC, nitrite did not ameliorate EIPH or exercise intolerance of obese rats, and did not change exercise-induced alteration in LVSP and LVEDP (Figure 4J, Figure 4B–C and Table VI in the Supplement). Taken together, these data identify an unexpected depletion of sGCβ1 enzyme in the pulmonary arteries of obese HFpEF rats, which fails to respond to NO donor or nitrite treatment *in vitro* and *in vivo*.

Similar to the observation in pulmonary artery homogenates, mRNA and protein levels of sGCβ1 were significantly decreased in PAVSMCs from obese rats and obese+sugen rats compared to cells from lean rats, suggesting reduced transcription of sGCβ1 (Figure 4K–L and Figure IV-D in the Supplement). We next surveyed transcription factors known to regulate sGCβ1, including Nuclear factor Y alpha (NFYA), HDAC3, and FoxO1, 3 and 4.[25,26,46] Notably, the mammalian CCAAT-box transcription factor NFY complex, composed of subunits Nuclear Factor YA (NFYA), Nuclear Factor YB (NFYB), and Nuclear Factor YC (NFYC), was previously reported to bind specifically to CCAAT-boxes in the sGCβ1 promoter.[27] Examination of the mRNA level of each target in PAVSMCs from lean, obese, and obese+sugen rats revealed that only NFYA was significantly decreased in obese and obese+sugen PAVSMCs (Figure 4K and Figure IV-D in the Supplement).

sGCβ1 levels were analyzed in primary PAVSMCs obtained from normal control humans and patients with diabetes (n=6 each). Control and diabetic patients were similar with respect to age, sex, and body mass index (Table VII in the Supplement). Patients with diabetes had higher fasting glucose levels and more therapy with oral anti-diabetic medicine, insulin utilization, statins, ARB/ACE-inhibitors, and Ca^{2+} blockers (Table VII in the Supplement). The expression of sGCβ1 protein was significantly decreased in PAVSMCs from diabetic patients when compared to control humans (Figure IV-E in the Supplement). Western blot analysis also revealed decreased NFYA expression in both nuclear and cytoplasmic extracts in rat and human diabetic PAVSMCs when compared with appropriate controls (lean rat or normal humans) (Figure 4L and Figure IV-F–G in the Supplement). Confirming a possible role of ROS in modulating NFYA and sGCβ1 expression, treatment with hydrogen peroxide (H_2O_2, 25μM, 24 hours) decreased NFYA and sGCβ1 expression in lean, obese, and obese+sugen PAVSMCs (Figure 4M). Superoxide dismutase (SOD, 400U/ml) and Catalase (1kU/ml) co-treatment, which metabolize ROS, significantly increased sGCβ1 and NFYA in lean and obese PAVSMCs (Figure IV-H in the Supplement). These studies of isolated pulmonary arteries and cultured PAVSMCs from HFpEF rat models and patients with diabetes, suggest that mitochondria generate ROS, which decreases NFYA levels and reduces transcription of sGCβ1, resulting in severely reduced sGC enzyme levels, which is unresponsive to endogenous and exogenous NO signaling.

Transcription factor NFYA controls sGC expression in PAVSMCs and is down regulated by metabolic stress and ROS

To assess the role of NFYA on sGCβ1 expression, cultured lean rat PAVSMCs were transfected NFYA siRNA. SiRNA-mediated knockdown of NFYA significantly reduced the protein (Figure 5A) and mRNA (data not shown) expression of NFYA and sGCβ1 while NFYA knockdown did not significantly change sGCα1, NFYB, and NYFC. To explore the mechanisms by which metabolic syndrome affects sGCβ1 expression, PAVSMCs were challenged with a media formulation (PGI) containing elevated fatty acids, glucose, and insulin. Lean treated with PGI media for 24 hours showed a temporal increase in cytoplasmic ROS (CellROX positive) (Figure 5B), while glutathione antioxidant factor (Thiol tracker positive) did not change in either group (Figure V-A in the Supplement). Similarly, PGI treatment for 24 hours increased mitochondrial ROS and membrane potential in control and diabetic rat PAVSMCs (Figure 5C). Treatment with MitoTEMPO (50μM, 10min) and rotenone (10μM, 10min) decreased PGI-induced ROS production in lean and obese PAVSMCs (Figure 5B), consistent with mitochondrial ROS formation. Furthermore, relative to appropriate control cells, lean PAVSMCs treated with PGI showed a similar and significant increase in mitochondrial complex I-IV activities and UCP2 expression without increases in ATP levels (Figure V-B in the Supplement), again supporting a mitochondrial source of ROS in response to PGI media. Moreover, while lean rat PAVSMCs cultured in PGI media decreased sGCβ1 and NFYA protein levels, co-treatment with SOD and Catalase attenuated these effects (Figure 5D). To further explore the transcriptional regulation of sGCβ1 by NFYA, chromatin immunoprecipitation (ChIP) was performed from PAVSMCs. Prior studies in hepatocytes reported that NFYA as part of the NFY complex, binds to the CCAAT box and regulates expression of sGCβ1.[25,29] Evaluation of the sGCβ1 promotor

reveals three CCAAT boxes, and three PCR primer sets were designed to span these regions for ChIP using anti-NFYA antibodies (Figure 5E and Table IX in the Supplement). PAVSMCs from lean and obese rats, and treated with PGI +/−SOD or catalase, were analyzed. Relative to the binding in lean PAVSMCs cultured in standard media, the binding of NFYA to sites #2 and #3 was decreased by PGI treatment in lean cells, and also decreased in obese PAVSMCs in standard media, and recovered with SOD and Catalase treatment (Figure 5F) in both cell culture systems. These results support a direct regulation of the sGCβ1 promotor activity by NFYA. We next performed bromouridine pulse-chase experiments to evaluate NFYA mRNA half-life and observed more rapid degradation of NFYA transcript in PAVSMCs from obese rats (Figure 5G). The addition of PGI or H_2O_2 to lean rat PAVSMCs accelerated the degradation of NFYA transcripts, which was rescued by the co-addition of the ROS scavengers SOD and catalase (Figure 5G). These data suggest that the transcription factor NFYA binds to sGCβ1 CCAAT boxes to increase enzyme expression in PAVSMCs and that metabolic syndrome causes ROS-dependent decay of NFYA mRNA, reducing NFYA expression and binding to the sGCβ1 promoter.

miR-193b promotes ROS-dependent degradation of NFYA, reducing sGCβ1 transcription

To explore the upstream mechanisms regulating NFYA expression, miR-193b expression was evaluated based on previous reports that patients with metabolic syndrome have higher miR-193b levels in plasma[33] and ectosomes,[47] and has been shown to negatively regulates NFYA expression in human adipocytes.[32] Relative to lean rats, miR-193b expression was increased in pulmonary arteries from both obese and obese+sugen rats (Figure 6A). Moreover, miR-193b expression was higher in obese rat cultured PAVSMCs relative to lean PAVSMCs, and PGI and H_2O_2 increased miR-193b expression in lean rat PAVSMCs, which was attenuated by SOD/Catalase co-treatment or mitoTEMPO treatment (Figure 6B). Consistent with this, PAVSMCs of patients with diabetes showed significantly increased miR-193b expression relative to control PAVSMCs (Figure VI-A in the Supplement). Separate analysis of each component of PGI revealed that both palmitic acid and glucose significantly increased miR-193b expression in lean PAVSMCs, while insulin alone did not (Figure VI-B in the Supplement). To confirm the interaction between miR-193b and NFYA, lean PAVSMCs were transfected with a plasmid construct encoding firefly luciferase and containing the 3’UTR sequence of NFYA (NFYA-Luc-3’UTR), and a miR-193b mimic or control miR. Luciferase activity in lean PAVSMCs expressing the NFYA-Luc-3’UTR was inhibited by addition of the miR-193b mimic (Figure VI-C in the Supplement), suggesting that miR-193b reduces the expression of NFYA in PAVSMCs through RNA degradation. PAVSMCs from lean and obese rats were next transfected with antago-miR-193b, which decreased miR-193 expression by 96% (Figure VI-D in the Supplement) and attenuated the degradation of NFYA and sGCβ1 mRNA and protein in obese rat PAVSMCs and lean rat PAVSMCs treated with PGI (Figure 6C–E). Moreover, miR-193b mimic significantly decreased sGCβ1 and NFYA expression in lean PAVSMCs (Figure VI-E in the Supplement). To explore the upstream mechanism, we evaluated the global H3K9 acetylation (H3K9ac, associated with activate promoters) in PAVSMCs. Relative to lean PAVSMCs, obese, obese+sugen PAVSMCs, or lean PAVSMCs treated with PGI showed higher levels of H3K9ac, which was attenuated by mitoTEMPO treatment (Figure 6F). To further investigate the mechanism for induction of miR-193b in obese PAVSMCs, ChIP assays were performed

so as to assess the presence H3K9ac, on the miR-193b promoter.[31] Three promoter regions (Sites #1–3) were predicted within the first 1000 base pair of the miR-193b proximal promoter as previously described (Figure 6G and Table IX in the Supplement).[31] Lean PAVSMCs treated with PGI or obese rat PAVSMCs showed higher levels of H3K9ac on miR-193b promoter regions, especially site at #2, which were attenuated by co-treatment with SOD and Catalase or mitoTEMPO treatment (Figure 6H). Together these data suggest that metabolic syndrome (or diabetes) increases miR-193b expression possibly by ROS-dependent H3K9 acetylation, enhancing NFYA transcript degradation, reducing NFYA expression, and leading to reduced sGCβ1 promoter activation and transcription (Figure 6I).

Forced NFYA expression in pulmonary arteries via AAV6 vector delivery improves PH and RV dysfunction during exercise in CpcPH model rats

To investigate whether forced NFYA expression restores sGCβ1 expression and improves PH, a recombinant adeno-associated virus (rAAV), carrying cDNA encoding the Human NFYA (hNFYA) long form coding sequence and containing an in-frame DDK tag was designed. At first, to select the appropriate rAAV serotype for our PAVSMCs and rats, rat PAVSMCs were exposed to several types of rAAV-GFP. rAAV serotype 6 showed the highest GFP expression intensity and transduction percentage in cultured rat PAVSMCs among rAAV serotype 2, 5, 6, 8, and 9 (Figure VII-A in the Supplement). Western blotting revealed double bands in the range of 40–50 kDa in obese PAVSMCs infected with rAAV6- NFYA-DDK; the lower size band is endogenous NFYA (44 kDa) and upper one is the 50 kDa NFYA-DDK fusion protein. Transduction with rAAV6-NFYA-DDK increased total NFYA (endogenous and fusion) expression in obese PAVSMCs compared to the cells with the rAAV6-GFP control vector, and significantly increased both DDK and sGCβ1 expression (Figure 7A). In addition, transduction with rAAV6-NFYA-DDK restored cGMP production induced by NONOate (10μM, 24 hours) in obese PAVSMCs compared to the cells infected with rAAV6-GFP (Figure 7B). Moreover, treatment with PGI decreased endogenous NFYA and sGCβ1 expression in lean PAVSMCs, which were partially restored by transduction of rAAV6-NFYA-DDK to express NFYA-DDK fusion protein (Figure VII-B in the Supplement). We note that NFYA expression could not be fully normalized with rAAV6-NFYA-DDK in the PGI model, likely reflecting persistent mRNA degradation by miR-193b (there is clearly more complete NFYA restoration with antagomiR-193b treatment in Figure 6F).

Next, the *in vivo* consequences of expressing NFYA in pulmonary smooth muscle cells of CpcPH rats was assessed. First, to establish the optimal delivery of the rAAV vector to the pulmonary arteries, the same amount of rAAV6-GFP vector (1.05×10^11 v.g.) was administrated to lean rats by direct delivery to pulmonary arteries via an implanted PE tube or intratracheal instillation 4-weeks prior to lung harvest and analysis (Figure VII-C in the Supplement). Immunofluorescent images revealed higher delivery of rAAV6-GFP to the pulmonary vasculature by pulmonary arterial administration rather than intratracheal instillation, that latter of which resulted in predominant airway epithelial treatment (Figure VII-D–F in the Supplement). Subsequently, ZSF-1 obese rats were treated with Sugen (100mg/kg) (CpcPH rats) at 8 weeks of age, and rAAV6-NFYA-DDK vector (1.05×10^11

v.g.) was administrated to the rats by pulmonary arterial injection at 17 weeks of age, 4 weeks prior to the hemodynamics analysis or organ harvest (Figure VII-C in the Supplement). Using this approach, NFYA expression in both CD31 and αSMA positive cells of pulmonary arteries were increased in CpcPH rats treated with rAAV6-NFYA-DDK compared to rats treated with rAAV6-GFP control (Figure 7C). Flow cytometric analysis showed higher DDK expression in both CD31 and αSMA positive cells of pulmonary arteries of CpcPH rats treated with rAAV6-NFYA-DDK (Figure 7D). Pulmonary arterial remodeling of CpcPH rats was not altered by treatment with rAAV6-NFYA-DDK (Figure VII-G in the Supplement) although NFYA has been reported to promote cellular proliferation in PAVSMCs.[28] Western blotting of pulmonary arteries demonstrated that sGCβ1, total NFYA (endogenous 44kDa and fusion 50kDa), and DDK expression (50kDa), were all increased in the rAAV6-NFYA-DDK infected group, while eNOS phosphorylation was not altered (Figure 7E). Moreover, cGMP plasma levels increased with rAAV6-NFYA-DDK treatment compared to rAAV6-GFP (Figure 7F). These data suggest that the rAAV6-NFYA-DDK vector increased NFYA expression and restored sGCβ1 levels and activity in PAVSMCs of CpcPH rats.

Transduction with rAAV6-NFYA-DDK reduced exercise-induced RVSP and RVEDP, and improved exercise-intolerance in CpcPH rats compared with rAAV6-GFP control, while LVSP or LVEDP were not altered (Figure 7G–H and Table X in the Supplement). Consistent with hemodynamic findings, ultrasonography evaluation showed that the exercise-induced RV dysfunction (dilated RVDd, decreased PAAT/ET ratio, and TAPSE), cardiac index (CI), and TPRi were all improved in the rAAV6-NFYA-DDK treated group while LV systolic and diastolic function were not altered (Figure 7I–K, Figure VIII-A and Table XI in the Supplement). Mechanistically, these data suggest that NFYA deficiency accounts for decreased sGC-cGMP signaling, pulmonary artery smooth muscle dysfunction, and EIPH in our severe CpcPH model (Figure VIII-B in the Supplement).

SGLT2 inhibition ameliorated metabolic syndrome in Obese rats treated with SU5416

In our EIPH and CpcPH models and in human PAVSMCs, metabolic syndrome appears to drive the upstream formation of mitochondrial ROS and miR-193b expression. This suggests that upstream control of the metabolic syndrome may represent an optimal therapeutic strategy; indeed, in our prior studies metformin had modest protective effects on PH in ZSF-1 rats treated with sugen. In addition to controlling diabetes and improving metabolic syndrome, SGLT2 inhibitor therapy is associated with decreases in heart failure related hospitalization, non-fatal myocardial infarction and cardiovascular death in adult patients with type 2 diabetes and cardio-vascular risk, and is currently being studied in clinical trials of human HFpEF (but not EIPH or CpcPH specifically).[37,38] To evaluate the effect of the SGLT2 inhibitor Empagliflozin on severe EIPH in CpcPH (obese+sugen) rats, eight weeks old obese rats received SU5416 (100mg/kg) once to induce PH, and Empagliflozin (10 mg/kg/day) via drinking water until 22 weeks old of age. Control groups included lean and obese rats treated with SU5416 only. At 21 weeks of age, rats were implanted with a 3 Fr catheter in the RV and LV, and at 22 weeks hemodynamics were evaluated during treadmill exercise protocols (Figure IX-A in the Supplement). Plasma samples from obese+sugen treated with empagliflozin were much less hyperlipidemic than samples from obese+sugen

rats (Figure IX-B in the Supplement). Obese+sugen rats treated with empagliflozin showed a significant improvement in metabolic syndrome endpoints, such as body weight (BW, g) (Figure 8A), HbA1c, insulin, insulin resistance (HOMA-iR), fasting glucose, glucose tolerance, and triglyceride levels (Figure 8B and Figure IX-C in the Supplement). As expected for treatment with a SGLT2 inhibitor, urinary glucose levels were much higher in obese+sugen treated with empagliflozin (Figure IX-D in the Supplement). Empagliflozin-treated obese+sugen rats showed reduced markers of oxidative stress. 4HNE and 8OHdG immunofluorescence staining around PAs, which was increased in obese+sugen rats relative to lean rats, was attenuated by treatment with empagliflozin (Figure 8C and Figure X-A in the Supplement). Similarly, resting oxLDL plasma levels, increased in obese+sugen rats, were reduced after treatment with empagliflozin (Figure X-B in the Supplement). Moreover, obese+sugen rats showed an exercise-induced increase in oxLDL plasma levels, which was not seen in obese+sugen treated with SGLT2 inhibitor (Figure X-B in the Supplement). Using mitochondria isolated from rat pulmonary arteries, mitochondrial complex I, III, IV activities, and UCP2 expression, were increased in obese+sugen rats relative to lean rats, but attenuated by treatment with empagliflozin (Figure X-C in the Supplement). Furthermore, empagliflozin treatment attenuated miR-193b expression in PAs of obese+sugen rats (Figure 8D). NFYA and sGCβ1 expression and H3K9 acetylation were improved by treatment with empagliflozin while eNOS expression of pulmonary arteries was not significantly altered (Figure 8E–F and Figure X-D in the Supplement). Consistent with the restored sGCβ1 expression, post-exercise cGMP levels were improved in treatment group (Figure 8G). These data suggest that treatment with empagliflozin may improve pulmonary arterial function of CpcPH rats through substantial improvement of sGC activity in the smooth muscle cell layer.

At rest, obese+sugen rats showed increased RVSP versus lean rats, which was not attenuated by treatment with empagliflozin (Figure 8H and Table XII in the Supplement). Consistent with the severity of this model, treatment with empagliflozin also did not improve resting LV function (EF, LV wall thickness, and cardiac output) and RV function (RVDd, TAPSE, and PAAT/ET) (Figure XI-A–C in the Supplement). However, during exercise (Ex), obese+sugen rats treated with empagliflozin showed improvement of exercise-induced increases in RVSP, RVEDP, LVEDP, and exercise intolerance (workload x BW) (Figure 8H–I). Post-exercise ultrasonography showed significant improvement of cardiac function (CO and CI) (Figure XI-B and Table XIII in the Supplement), RV function (RVDd, PAAT/ET and TAPSE) (Figure VIII-K in the Supplement) and TPRi (Figure XI-D in the Supplement) in obese+sugen rats treated with empagliflozin. MR imaging was used to assess the effect of empagliflozin on the impaired PA response of obese+sugen rats to dobutamine challenge. Relative to the untreated Obese+sugen group, rats treated with empagliflozin showed significant improvement of PA dilation and less RV dilation (Figure 8J). These data suggest that SGLT2 inhibition improves metabolic syndrome and reduces mitochondrial ROS generation, enhances sGC-cGMP signaling and improves PA vasodilatory function during exercise. These improvements of cardiopulmonary function by SGLT2 inhibitor contributed to the improvement of EIPH in CpcPH model rats (Figure XII in the Supplement).

Discussion

The current study evaluates two novel rodent models of HFpEF and pulmonary hypertension during exercise. The first model is EIPH in HFpEF (the ZSF-1 obese rat without sugen treatment), characterized by normal resting pulmonary pressures that rise significantly during treadmill exercise. The second is a CpcPH model (the ZSF-1 obese rat with sugen treatment), with resting pulmonary hypertension and pulmonary vascular remodeling, and significant worsening of RV dysfunction during exercise. These models recapitulate the human phenotype of PH in the setting of HFpEF and capture a spectrum of the severity of disease and impaired functional capacity. In these studies, MR imaging of pulmonary arteries revealed impaired pulmonary arterial vasodilatory reserve during dobutamine challenge in obese rats, with and without sugen treatment. An unexpected and central molecular feature of the pulmonary vasculopathy relates to reduced transcription and expression of PAVSMC sGCβ1 with reduced cGMP signaling, caused by a reduction in the transcription factor NFYA. This pathophysiology appears to be initiated by metabolic syndrome-mediated increases in mitochondrial ROS, which increase miR-193b levels, driving NFYA mRNA degradation and reduced sGCβ1 transcription. Interestingly, a homologous pathophysiology was observed in PAVSMCs from diabetic humans, could be induced by driving cellular insulin resistance by exposure of lean PAVSM cells to PGI treatment, and was restored with in all cell culture models through scavenging of mitochondrial ROS or inhibition of miR-193b. Moreover, forced NFYA expression in pulmonary artery vascular smooth muscle via AAV6 transgene delivery restores sGC-cGMP signaling, and rescued the exercise-induced alteration in PH and RV dysfunction in CpcPH rats. Finally, an SGLT2 inhibitor also decreased miR-193b levels, restored NFYA and sGCβ1 expression, and improved exercise PH in obese rats with CpcPH.

We have previously published that treating the ZSF-1 obese rat with sugen, a VEGF receptor blocker, induces a double hit (metabolic syndrome with vascular injury) that leads to PH in the setting of HFpEF (CpcPH). Obese ZSF-1 rats showed higher LVEDP and mPAP consistent with post capillary PH in the setting of HFpEF. These obese ZSF-1 rats treated with sugen demonstrate PA remodeling and elevated PA resistance characterized by a higher TPRi, consistent with pre- and post-capillary PH (a CpcPH model). In the current studies we explore the additional stress of exercise on the ZSF-1 rat without and with sugen. Importantly, the ZSF-1 rats without sugen do not develop PH at rest but do develop PH with exercise, essentially modeling EIPH. The addition of sugen leads to PH at rest and more severe EIPH with greater RV dysfunction, modeling the more advanced state of CpcPH. Rest and exercise doppler-echocardiographic measurements in these models reveal normal ejection fraction (EF), low E/A ratio consistent with diastolic dysfunction, and low cardiac index (CI) and tricuspid anulus plane systolic excursion (TAPSE) with exercise, indicating the worsening right ventricular function with exercise in these 2 models. These data suggest that we have developed robust models of EIPH (ZSF-1 without sugen), and HFpEF with CpcPH (ZSF-1 rat treated with sugen).

Changes in pulmonary pressure with HFpEF during exercise relate to both increases in left ventricular end-diastolic pressure as well as pulmonary vasoconstriction or a failure to vasodilate. In order to evaluate this directly, we evaluated the diameter of the pulmonary

arteries (PA) with MRI during dobutamine challenge. The data suggest that in the CpcPH model there is resting PH resulting in chronic increases in PA diameter, consistent with observations in human disease, but also a profound failure to vasodilate (measured as a reduction in the change in PA area from diastole to systole) as cardiac output is increased with dobutamine, with even greater compromise evident in the sugen treated ZSF-1 obese rat (CpcPH model).

While the CpcPH model is more severe with resting PH and evident pulmonary vascular hypertrophy, the EIPH model does develop pulmonary vascular dysfunction that becomes evident during dobutamine challenge by MRI and is also observed in studies of isolated pulmonary vessel myography. Myographic analysis of PAs reveal an impaired vasodilatory response to acetylcholine and sodium nitroprusside in the EIPH models, consistent with molecular observations of sGCβ1 depletion in PAVSMCs. Interestingly, both models of EIPH and CpcPH exhibit similar profound impairments in sGCβ1 expression with reduced cGMP levels, despite more severe PH at rest and exercise in the CpcPH model. The difference in severity may arise from the development of additional pulmonary vascular cellular remodeling, such as PAVSMC proliferation and increased baseline rest PH, in the CpcPH model, with more severe PH and RV dysfunction evident with exercise. Considering these data, we propose that the EIPH model rats exhibit functional PA impairments even without pathologically evident pulmonary arterial remodeling. This latent functional PA impairment becomes manifest during exercise or dobutamine stress.

The regulation of pulmonary artery relaxation is in large part mediated through production of cGMP by sGC in PAVSMCs. PDE5 inhibitor are well-known to improve the cardio-pulmonary function of patients with HFpEF and in rodent HFpEF rodent models and have the possibility to improve cGMP level and EIPH in HFpEF or CpcPH models.[48] However, a relative decrease of plasma cGMP in exercised obese rats, preserved PDE5 expression, poor responses of cultured PAVSMCs to NO donors, sGC stimulator and activator, and decreased expression of pulmonary artery sGCβ1 at the transcript and protein level, led us to examine regulation of sGCβ1 expression in PAVSMCs isolated from lean and obese rats, with and without sugen treatment. Examination of known transcription factors shown to regulated sGCβ1 expression in other cell types revealed a marked decrease in NFYA expression at both the RNA and protein levels in obese PAVSMCs. siRNA mediated knockdown of NFYA in PAVSMCs led to decreased sGCβ1 expression, suggesting that NFYA regulates sGCβ1 expression in PAVSMCs. While we do not have PAVSMCs from patients with HFpEF, we observed similar decreases in sGCβ1 and NFYA expression in PAVSMCs isolated from patients with diabetes and lean rat cells treated with PGI to induce a metabolic syndrome phenotype. These concordant results suggest that pathophysiologic processes of metabolic syndrome in both obese rats and diabetic patients are associated with reduced expression of NFYA, which appears to be the dominant transcription factor in PAVSMCs that regulates sGCβ1 expression.

Abnormal or inappropriate ROS mediates many pathophysiologic processes of the metabolic syndrome[35], and this study demonstrated evidence for elevated ROS in pulmonary vasculature of obese rats. Culture of lean rat PAVSMCs in a metabolic-syndrome-mimic media increased mitochondrial complex activities and ROS production. The generation

of mitochondrial ROS, *in vivo* and in our cell culture systems, led to increased levels of miR-193b which targets and degrades NFYA mRNA.[32] Previous reports demonstrated that patients with metabolic syndrome have higher miR-193b levels in plasma[33] and ectosomes.[47] Moreover, miR-193b has been shown to negatively regulate NFYA expression in human adipocytes.[32] In addition to regulating sGCβ1 expression, NYFA also regulates gluconeogenesis genes induced by glucagon stimulation and fasting *in vivo*.[29] Furthermore, NFYA knockout mice exhibit lower leptin expression and higher glucose, insulin, and triglyceride levels[49], suggesting an important role for miR-193b and NFYA expression in regulating metabolic syndrome pathophysiology. These findings suggest that metabolic syndrome, through enhanced mitochondrial ROS, drive miR-193b-dependent down-regulation of NFYA/sGCβ1 expression, and consequent pulmonary arterial dysfunction.

To investigate if NFYA degradation determines our observed EIPH phenotypes, we attempted to rescue NFYA expression using AAV gene delivery approaches. Treatment of severe CpcPH (obese+sugen) rats with rAAV6-NFYA-DDK increased pulmonary artery NFYA and sGCβ1 expression and increased cGMP levels, which led to the diminution of EIPH (reduced exercise-induced RVSP elevation). The AAV gene delivery forced NFYA expression not only in pulmonary smooth muscle, but also endothelium. However, considering the smooth-muscle-specific-expression of sGCβ1, the functional importance of AAV-induced NFYA expression is most likely through increased sGCβ1 expression in PAVSM cells. These experiments suggest a causal role of NFYA in the control of sGCβ1 and in the development of EIPH and CpcPH, and also define a novel therapeutic approach to the treatment of PH in the setting of HFpEF.

The major finding of this paper is that metabolic syndrome down-regulates sGC expression in pulmonary artery vascular smooth muscle cells, representing an up-stream mechanism of impaired pulmonary artery vasodilation in EIPH. Since sGC is the target for NO signaling, a reduced sGC enzyme level decreases the responsiveness to sGC activation by NO and NO donors (nitrite), potentially explaining a failure of drugs like nitrite, nitroglycerin, phosphodiesterase 5 inhibitors, and sGC stimulators in the setting of HFpEF. Moreover, our data suggest that pulmonary arterial dysfunction, caused by metabolic syndrome and reduced sGC expression, coupled with higher LVEDP, contributes to the development of EIPH. As treatment with SGLT2 inhibitors has been reported to improve metabolic syndrome, blood pressure and fluid retention, we tested the effect of empagliflozin in our CpcPH (obese+sugen) rats. CpcPH model rats treated with empagliflozin showed highly significant improvements in metabolic syndrome endpoints, associated with the amelioration of PH and RV dysfunction during exercise. SGLT2 inhibitor also attenuated H3K9 acetylation and miR-193b expression, which restored pulmonary artery NFYA-sGCβ1 signaling, and ameliorated dobutamine-induced pulmonary arterial dysfunction. As phosphorylation of pulmonary artery eNOS was not improved by treatment with SGLT2 inhibitor, we propose that the improvement of pulmonary arterial function and EIPH arises from the restored sGCβ1 expression. These data are consistent with the recent publication of human data in Circulation showing that SGLT-2 inhibitors reduce pulmonary pressures in patients with heart failure, including HFpEF.[50]

With therapeutic enhancement of the NFYA-sGCβ1-cGMP signaling axis in our CpcPH model with SGLT-2 inhibitors or rAAV6-NFYA-DDK gene delivery, there is improvement in exercise induced pulmonary hypertension and improved exercise capacity, but this therapy does not reverse the pathological remodeling. This is consistent with similar reductions in NFYA-sGCβ1 signaling in the ZSF-1 rat with and without sugen treatment and the greater anatomical remodeling observed with sugen treatment that may not be corrected with enhanced sGCβ1-cGMP signaling.

Limitations

Several potential limitations are acknowledged in the present studies: 1) Our MRI and biochemical studies analyzed only the second order branches of the rat pulmonary arteries. Thus the contribution of functional and biochemical changes in more distal pulmonary arteries are not evaluated; 2) Similarly, for technical reasons, cultured cell work utilized PAVSMCs from the main branch of rat pulmonary arteries. Other cells types, or cells derived from other regions of the pulmonary arterial tree, could reveal additional mechanisms; 3) Biochemical analyses of acutely isolated pulmonary artery tissues may not present the same biochemical processes identified in cultured PAVSMCs, and the PGI media may not mimic the full ‘milieu’ of circulating factors within a rat or human with metabolic syndrome; 4) To relate findings from PAVSMCs isolated from rats with metabolic syndrome and HFpEF (ZSF-1/obese) to humans, our investigations were limited to PAVSMCs from diabetic humans as PAVSMCs from patients with HFpEF were not available; 5) The data from the SGLT2 inhibitor studies shows increases in PAVSMC NFYA and sGCβ1 expression associated with improved PH, however the causal role of NFYA in mediating the clinical effects of SGLT2 inhibition is not definitive. However, a causal role of NFYA is supported by the AAV-mediated NFYA-overexpression studies.

In conclusion, we present two novel models of EIPH and CpcPH developed in obese ZSF-1 rats with HFpEF and metabolic syndrome, characterized by PA dysfunction and exercise-induced alterations in cardiac function resembling that reported for human patients. A central finding is the reduced expression in PAVSMCs of the transcription factor NFYA, which critically regulates sGCβ1 expression and PA function. Our studies provide evidence that forced expression of NFYA or upstream inhibition of the metabolic syndrome with the SGLT2 inhibitor improves exercise PH in our severe CpcPH model, accompanied by improvements in the NYFA-sGC-cGMP signaling pathway. These results provide new mechanistic insights into the relationship between metabolic syndrome, EIPH, and HFpEF, and suggest new therapeutic approaches targeting metabolic syndrome, mitochondrial ROS and a miR-193b-NFYA-sGC axis.

Supplementary Material

Refer to Web version on PubMed Central for supplementary material.

Acknowledgments

We are grateful to the lab members of the Pittsburgh Heart, Lung and Blood Vascular Medicine Institute in the University of Pittsburgh School of Medicine. We thank the following for their expert advice and access to instrumentation; the University of Pittsburgh Heart Lung and Blood Vascular Medicine Institute Animal Small

Animal Hemodynamic Core, and Small Animal Ultrasonography Core; University of Pittsburgh Center for Biologic Imaging; the Children's Hospital of Pittsburgh Rangos Research Center Animal Imaging Core; and the University of Pittsburgh Department of Immunology United Flow Cores.

Sources of Funding

This study was supported by funds from the NIH (NIH; 5P01HL10345509, Gladwin PI (principal investigator); S10OD023684, Kang Kim PI; R01 HL 133864, R01 HL 128304, Straub PI; R21-EB023507, Wu PI; R01 HL142932 and HL117917, St Hilaire PI; R01 HL133003-01A1, Shiva PI; R01 HL146465, Gomez PI; R01 HL113178 and R01 HL130261, Goncharova PI; R01HL142638, Lai PI),; R01HL124021, HL122596, HL138437, and UH2/UH3 TR002073, Chan PI), American Heart Association (AHA) (18CDA34140024, Wu PI), (AHA Established Investigator Grant 19 EIA34770095, Straub PI; AHA Established Investigator Grant 18EIA33900027, Chan PI), US Dept of Defense (W81XWH1810070, Wu PI), Children's Hospital of Pittsburgh (CHP00-CY19 RAC, Wu PI), the Uehara memorial foundation postdoctoral fellowship (Taijyu Satoh), and China Council Scholarship (CSC201706370266, Longfei Wang).

Disclosures

Dr. Gladwin is a co-inventor of patents and patent applications directed to the use of recombinant neuroglobin and heme-based molecules as antidotes for CO poisoning, which have been licensed by Globin Solutions, Inc. Dr. Gladwin is a shareholder, advisor, and director in Globin Solutions, Inc. Dr. Gladwin is also co-inventor on patents directed to the use of nitrite salts in cardiovascular diseases, which were previously licensed to United Therapeutics, and is now licensed to Globin Solutions and Hope Pharmaceuticals. Dr. Gladwin is a principal-investigator in a research collaboration with Bayer Pharmaceuticals to evaluate riociguat as a treatment for patients with SCD. Dr. Gladwin has served as a consultant for Epizyme, Inc., Actelion Clinical Research, Inc., Acceleron Pharma, Inc., Catalyst Biosciences, Inc., Modus Therapeutics, Sujana Biotech, LLC, Complexa Inc., Pfizer Inc., and United Therapeutics Corporation. Dr. Gladwin is also on Bayer HealthCare LLC's Heart and Vascular Disease Research Advisory Board. Dr. Chan has served as a consultant for Zogenix, Aerpio, and United Therapeutics; Dr. Chan has held research grants from Actelion and Pfizer. Dr McTiernan is a shareholder in Globin Solutions.

Non-standard Abbreviations and Acronyms

αSMA	α-smooth muscle actin
cGMP	Cyclic 3'−5' guanosine monophosphate
GTT	Glucose Tolerance Test
HOMA-iR	Homeostasis Model Assessment-insulin Resistance
EIPH	Exercise-induced pulmonary hypertension
ET	Ejection time
HFpEF	Heart Failure with preserved Ejection Fraction
LVEDP	Left ventricular end-diastolic pressure
MRI	Magnetic resonance imaging
NFYA	Nuclear factor Y alpha subunit
NFYB	Nuclear factor Y B subunit
NFYC	Nuclear factor Y C subunit
PA	Pulmonary artery
PAAT	Pulmonary artery acceleration time
PAVSMC	Pulmonary artery vascular smooth muscle cell

PH	Pulmonary hypertension
RVH	Right ventricular hypertrophy
rAAV	Recombinant adeno-associated viral vector
ROS	Reactive oxygen species
RVSP	Right ventricular systolic pressure
sGCβ1	Soluble guanylate cyclase β1 subunit
TAPSE	Tricuspid annular plane systolic excursion
TPRi (RVSP/CI)	Total pulmonary artery resistance index

References

1. Levine AR, Simon MA and Gladwin MT. Pulmonary vascular disease in the setting of heart failure with preserved ejection fraction. Trends Cardiovasc Med. 2019;29:207–217. doi: 10.1016/j.tcm.2018.08.005. [PubMed: 30177249]
2. Lai YC, Wang L and Gladwin MT. Insights into the pulmonary vascular complications of heart failure with preserved ejection fraction. J Physiol. 2019;597:1143–1156. doi: 10.1113/JP275858. [PubMed: 30549058]
3. Benjamin EJ, Virani SS, Callaway CW, Chamberlain AM, Chang AR, Cheng S, Chiuve SE, Cushman M, Delling FN, Deo R, de Ferranti SD, Ferguson JF, Fornage M, Gillespie C, Isasi CR, Jimenez MC, Jordan LC, Judd SE, Lackland D, Lichtman JH, Lisabeth L, Liu S, Longenecker CT, Lutsey PL, Mackey JS, Matchar DB, Matsushita K, Mussolino ME, Nasir K, O'Flaherty M, Palaniappan LP, Pandey A, Pandey DK, Reeves MJ, Ritchey MD, Rodriguez CJ, Roth GA, Rosamond WD, Sampson UKA, Satou GM, Shah SH, Spartano NL, Tirschwell DL, Tsao CW, Voeks JH, Willey JZ, Wilkins JT, Wu JH, Alger HM, Wong SS, Muntner P, American Heart Association Council on E, Prevention Statistics C and Stroke Statistics S. Heart Disease and Stroke Statistics-2018 Update: A Report From the American Heart Association. Circulation. 2018;137:e67–e492. doi: 10.1161/CIR.0000000000000558. [PubMed: 29386200]
4. Dunlay SM, Roger VL and Redfield MM. Epidemiology of heart failure with preserved ejection fraction. Nat Rev Cardiol. 2017;14:591–602. doi: 10.1038/nrcardio.2017.65. [PubMed: 28492288]
5. Reddy YNV, Carter RE, Obokata M, Redfield MM and Borlaug BA. A Simple, Evidence-Based Approach to Help Guide Diagnosis of Heart Failure With Preserved Ejection Fraction. Circulation. 2018;138:861–870. doi: 10.1161/CIRCULATIONAHA.118.034646. [PubMed: 29792299]
6. Galie N, Humbert M, Vachiery JL, Gibbs S, Lang I, Torbicki A, Simonneau G, Peacock A, Vonk Noordegraaf A, Beghetti M, Ghofrani A, Gomez Sanchez MA, Hansmann G, Klepetko W, Lancellotti P, Matucci M, McDonagh T, Pierard LA, Trindade PT, Zompatori M, Hoeper M and Group ESCSD. 2015 ESC/ERS Guidelines for the diagnosis and treatment of pulmonary hypertension: The Joint Task Force for the Diagnosis and Treatment of Pulmonary Hypertension of the European Society of Cardiology (ESC) and the European Respiratory Society (ERS): Endorsed by: Association for European Paediatric and Congenital Cardiology (AEPC), International Society for Heart and Lung Transplantation (ISHLT). Eur Heart J. 2016;37:67–119. doi: 10.1093/eurheartj/ehv317. [PubMed: 26320113]
7. Lai YC, Potoka KC, Champion HC, Mora AL and Gladwin MT. Pulmonary arterial hypertension: the clinical syndrome. Circ Res. 2014;115:115–130. doi: 10.1161/CIRCRESAHA.115.301146. [PubMed: 24951762]
8. Borlaug BA, Kane GC, Melenovsky V and Olson TP. Abnormal right ventricular-pulmonary artery coupling with exercise in heart failure with preserved ejection fraction. Eur Heart J. 2016;37:3293–3302. doi: 10.1093/eurheartj/ehw241.

9. Borlaug BA, Nishimura RA, Sorajja P, Lam CS and Redfield MM. Exercise hemodynamics enhance diagnosis of early heart failure with preserved ejection fraction. Circ Heart Fail. 2010;3:588–595. doi: 10.1161/CIRCHEARTFAILURE.109.930701. [PubMed: 20543134]

10. Borlaug BA. Evaluation and management of heart failure with preserved ejection fraction. Nat Rev Cardiol. 2020;17:559–573. doi: 10.1038/s41569-020-0363-2. [PubMed: 32231333]

11. Reddy YNV, Olson TP, Obokata M, Melenovsky V and Borlaug BA. Hemodynamic correlates and diagnostic role of cardiopulmonary exercise testing in heart failure with preserved ejection fraction. JACC Heart Fail. 2018;6:665–675. doi: 10.1016/j.jchf.2018.03.003. [PubMed: 29803552]

12. Hoeper MM, Barbera JA, Channick RN, Hassoun PM, Lang IM, Manes A, Martinez FJ, Naeije R, Olschewski H, Pepke-Zaba J, Redfield MM, Robbins IM, Souza R, Torbicki A and McGoon M. Diagnosis, assessment, and treatment of non-pulmonary arterial hypertension pulmonary hypertension. J Am Coll Cardiol. 2009;54:S85–96. doi: 10.1016/j.jacc.2009.04.008. [PubMed: 19555862]

13. Kovacs G, Herve P, Barbera JA, Chaouat A, Chemla D, Condliffe R, Garcia G, Grunig E, Howard L, Humbert M, Lau E, Laveneziana P, Lewis GD, Naeije R, Peacock A, Rosenkranz S, Saggar R, Ulrich S, Vizza D, Vonk Noordegraaf A and Olschewski H. An official European Respiratory Society statement: pulmonary haemodynamics during exercise. Eur Respir J. 2017;50. doi: 10.1183/13993003.00578-2017.

14. Rosenkranz S, Gibbs JS, Wachter R, De Marco T, Vonk-Noordegraaf A and Vachiery JL. Left ventricular heart failure and pulmonary hypertension. Eur Heart J. 2016;37:942–954. doi: 10.1093/eurheartj/ehv512. [PubMed: 26508169]

15. Vanderpool RR, Saul M, Nouraie M, Gladwin MT and Simon MA. Association between hemodynamic markers of pulmonary hypertension and outcomes in heart failure with preserved ejection fraction. JAMA Cardiol. 2018;3:298–306. doi: 10.1001/jamacardio.2018.0128. [PubMed: 29541759]

16. Gerges M, Gerges C, Pistritto AM, Lang MB, Trip P, Jakowitsch J, Binder T and Lang IM. Pulmonary Hypertension in Heart Failure. Epidemiology, Right Ventricular Function, and Survival. Am J Respir Crit Care Med. 2015;192:1234–1246. doi: 10.1164/rccm.201503-0529OC. [PubMed: 26181215]

17. Gorter TM, Obokata M, Reddy YNV, Melenovsky V and Borlaug BA. Exercise unmasks distinct pathophysiologic features in heart failure with preserved ejection fraction and pulmonary vascular disease. Eur Heart J. 2018;39:2825–2835. doi: 10.1093/eurheartj/ehy331. [PubMed: 29947750]

18. Mohammed SF, Hussain I, AbouEzzeddine OF, Takahama H, Kwon SH, Forfia P, Roger VL and Redfield MM. Right ventricular function in heart failure with preserved ejection fraction: a community-based study. Circulation. 2014;130:2310–2320. doi: 10.1161/CIRCULATIONAHA.113.008461. [PubMed: 25391518]

19. Opitz CF, Hoeper MM, Gibbs JS, Kaemmerer H, Pepke-Zaba J, Coghlan JG, Scelsi L, D'Alto M, Olsson KM, Ulrich S, Scholtz W, Schulz U, Grunig E, Vizza CD, Staehler G, Bruch L, Huscher D, Pittrow D and Rosenkranz S. Pre-capillary, combined, and post-capillary pulmonary hypertension: A pathophysiological continuum. J Am Coll Cardiol. 2016;68:368–378. doi: 10.1016/j.jacc.2016.05.047. [PubMed: 27443433]

20. Schiattarella GG, Altamirano F, Tong D, French KM, Villalobos E, Kim SY, Luo X, Jiang N, May HI, Wang ZV, Hill TM, Mammen PPA, Huang J, Lee DI, Hahn VS, Sharma K, Kass DA, Lavandero S, Gillette TG and Hill JA. Nitrosative stress drives heart failure with preserved ejection fraction. Nature. 2019;568:351–356. doi: 10.1038/s41586-019-1100-z. [PubMed: 30971818]

21. Lai YC, Tabima DM, Dube JJ, Hughan KS, Vanderpool RR, Goncharov DA, St Croix CM, Garcia-Ocana A, Goncharova EA, Tofovic SP, Mora AL and Gladwin MT. SIRT3-AMP-activated protein kinase activation by nitrite and metformin improves hyperglycemia and normalizes pulmonary hypertension associated with heart failure with preserved ejection Fraction. Circulation. 2016;133:717–731. doi: 10.1161/CIRCULATIONAHA.115.018935. [PubMed: 26813102]

22. Tejero J, Shiva S and Gladwin MT. Sources of vascular nitric oxide and reactive oxygen species and their regulation. Physiol Rev. 2019;99:311–379. doi: 10.1152/physrev.00036.2017. [PubMed: 30379623]

23. Guzik TJ, Mussa S, Gastaldi D, Sadowski J, Ratnatunga C, Pillai R and Channon KM. Mechanisms of increased vascular superoxide production in human diabetes mellitus: role of

NAD(P)H oxidase and endothelial nitric oxide synthase. Circulation. 2002;105:1656–1662. doi: 10.1161/01.cir.0000012748.58444.08. [PubMed: 11940543]

24. Rahaman MM, Nguyen AT, Miller MP, Hahn SA, Sparacino-Watkins C, Jobbagy S, Carew NT, Cantu-Medellin N, Wood KC, Baty CJ, Schopfer FJ, Kelley EE, Gladwin MT, Martin E and Straub AC. Cytochrome b5 reductase 3 modulates soluble guanylate cyclase redox state and cGMP signaling. Circ Res. 2017;121:137–148. doi: 10.1161/CIRCRESAHA.117.310705. [PubMed: 28584062]
25. Sharina IG, Martin E, Thomas A, Uray KL and Murad F. CCAAT-binding factor regulates expression of the beta1 subunit of soluble guanylyl cyclase gene in the BE2 human neuroblastoma cell line. Proc Natl Acad Sci U S A. 2003;100:11523–11528. doi: 10.1073/pnas.1934338100. [PubMed: 14504408]
26. Galley JC, Durgin BG, Miller MP, Hahn SA, Yuan S, Wood KC and Straub AC. Antagonism of Forkhead box subclass O transcription factors elicits loss of soluble guanylyl cyclase expression. Mol Pharmacol. 2019;95:629–637. doi: 10.1124/mol.118.115386. [PubMed: 30988014]
27. Belluti S, Semeghini V, Basile V, Rigillo G, Salsi V, Genovese F, Dolfini D and Imbriano C. An autoregulatory loop controls the expression of the transcription factor NF-Y. Biochim Biophys Acta Gene Regul Mech. 2018;1861:509–518. doi: 10.1016/j.bbagrm.2018.02.008. [PubMed: 29505822]
28. Silvestre-Roig C, Fernandez P, Esteban V, Pello OM, Indolfi C, Rodriguez C, Rodriguez-Calvo R, Lopez-Maderuelo MD, Bauriedel G, Hutter R, Fuster V, Ibanez B, Redondo JM, Martinez-Gonzalez J and Andres V. Inactivation of nuclear factor-Y inhibits vascular smooth muscle cell proliferation and neointima formation. Arterioscler Thromb Vasc Biol. 2013;33:1036–1045. doi: 10.1161/ATVBAHA.112.300580. [PubMed: 23430616]
29. Zhang Y, Guan Q, Liu Y, Zhang Y, Chen Y, Chen J, Liu Y and Su Z. Regulation of hepatic gluconeogenesis by nuclear factor Y transcription factor in mice. J Biol Chem. 2018;293:7894–7904. doi: 10.1074/jbc.RA117.000508. [PubMed: 29530977]
30. Meloche J, Pflieger A, Vaillancourt M, Paulin R, Potus F, Zervopoulos S, Graydon C, Courboulin A, Breuils-Bonnet S, Tremblay E, Couture C, Michelakis ED, Provencher S and Bonnet S. Role for DNA damage signaling in pulmonary arterial hypertension. Circulation. 2014;129:786–797. doi: 10.1161/CIRCULATIONAHA.113.006167. [PubMed: 24270264]
31. Yu Q, Tai YY, Tang Y, Zhao J, Negi V, Culley MK, Pilli J, Sun W, Brugger K, Mayr J, Saggar R, Saggar R, Wallace WD, Ross DJ, Waxman AB, Wendell SG, Mullett SJ, Sembrat J, Rojas M, Khan OF, Dahlman JE, Sugahara M, Kagiyama N, Satoh T, Zhang M, Feng N, Gorcsan J 3rd, Vargas SO, Haley KJ, Kumar R, Graham BB, Langer R, Anderson DG, Wang B, Shiva S, Bertero T and Chan SY. BOLA (BolA Family Member 3) Deficiency Controls Endothelial Metabolism and Glycine Homeostasis in Pulmonary Hypertension. Circulation. 2019;139:2238–2255. doi: 10.1161/CIRCULATIONAHA.118.035889. [PubMed: 30759996]
32. Belarbi Y, Mejhert N, Lorente-Cebrian S, Dahlman I, Arner P, Ryden M and Kulyte A. MicroRNA-193b controls adiponectin production in human white adipose tissue. J Clin Endocrinol Metab. 2015;100:E1084–1088. doi: 10.1210/jc.2015-1530. [PubMed: 26020766]
33. Parrizas M, Brugnara L, Esteban Y, Gonzalez-Franquesa A, Canivell S, Murillo S, Gordillo-Bastidas E, Cusso R, Cadefau JA, Garcia-Roves PM, Servitja JM and Novials A. Circulating miR-192 and miR-193b are markers of prediabetes and are modulated by an exercise intervention. J Clin Endocrinol Metab. 2015;100:E407–415. doi: 10.1210/jc.2014-2574. [PubMed: 25532038]
34. Wang S, Lincoln TM and Murphy-Ullrich JE. Glucose downregulation of PKG-I protein mediates increased thrombospondin1-dependent TGF-beta activity in vascular smooth muscle cells. Am J Physiol Cell Physiol. 2010;298:C1188–1197. doi: 10.1152/ajpcell.00330.2009. [PubMed: 20164378]
35. Liu S, Ma X, Gong M, Shi L, Lincoln T and Wang S. Glucose down-regulation of cGMP-dependent protein kinase I expression in vascular smooth muscle cells involves NAD(P)H oxidase-derived reactive oxygen species. Free Radic Biol Med. 2007;42:852–863. doi: 10.1016/j.freeradbiomed.2006.12.025. [PubMed: 17320767]
36. Redfield MM, Chen HH, Borlaug BA, Semigran MJ, Lee KL, Lewis G, LeWinter MM, Rouleau JL, Bull DA, Mann DL, Deswal A, Stevenson LW, Givertz MM, Ofili EO, O'Connor CM, Felker GM, Goldsmith SR, Bart BA, McNulty SE, Ibarra JC, Lin G, Oh JK, Patel MR, Kim RJ,

Tracy RP, Velazquez EJ, Anstrom KJ, Hernandez AF, Mascette AM, Braunwald E and Trial R. Effect of phosphodiesterase-5 inhibition on exercise capacity and clinical status in heart failure with preserved ejection fraction: a randomized clinical trial. JAMA. 2013;309:1268–1277. doi: 10.1001/jama.2013.2024. [PubMed: 23478662]

37. Fitchett D, Zinman B, Wanner C, Lachin JM, Hantel S, Salsali A, Johansen OE, Woerle HJ, Broedl UC, Inzucchi SE and investigators E-ROt. Heart failure outcomes with empagliflozin in patients with type 2 diabetes at high cardiovascular risk: results of the EMPA-REG OUTCOME(R) trial. Eur Heart J. 2016;37:1526–1534. doi: 10.1093/eurheartj/ehv728. [PubMed: 26819227]
38. Mahaffey KW, Neal B, Perkovic V, de Zeeuw D, Fulcher G, Erondu N, Shaw W, Fabbrini E, Sun T, Li Q, Desai M, Matthews DR and Group CPC. Canagliflozin for primary and secondary prevention of cardiovascular events: Results from the CANVAS program (Canagliflozin Cardiovascular Assessment Study). Circulation. 2018;137:323–334. doi: 10.1161/CIRCULATIONAHA.117.032038. [PubMed: 29133604]
39. He C, Bassik MC, Moresi V, Sun K, Wei Y, Zou Z, An Z, Loh J, Fisher J, Sun Q, Korsmeyer S, Packer M, May HI, Hill JA, Virgin HW, Gilpin C, Xiao G, Bassel-Duby R, Scherer PE and Levine B. Exercise-induced BCL2-regulated autophagy is required for muscle glucose homeostasis. Nature. 2012;481:511–515. doi: 10.1038/nature10758. [PubMed: 22258505]
40. Goncharov DA, Kudryashova TV, Ziai H, Ihida-Stansbury K, DeLisser H, Krymskaya VP, Tuder RM, Kawut SM and Goncharova EA. Mammalian target of rapamycin complex 2 (mTORC2) coordinates pulmonary artery smooth muscle cell metabolism, proliferation, and survival in pulmonary arterial hypertension. Circulation. 2014;129:864–874. doi: 10.1161/CIRCULATIONAHA.113.004581. [PubMed: 24270265]
41. Hamdani N, Franssen C, Lourenco A, Falcao-Pires I, Fontoura D, Leite S, Plettig L, Lopez B, Ottenheijm CA, Becher PM, Gonzalez A, Tschope C, Diez J, Linke WA, Leite-Moreira AF and Paulus WJ. Myocardial titin hypophosphorylation importantly contributes to heart failure with preserved ejection fraction in a rat metabolic risk model. Circ Heart Fail. 2013;6:1239–1249. doi: 10.1161/CIRCHEARTFAILURE.113.000539. [PubMed: 24014826]
42. Teixeira-Coelho F, Fonseca CG, Barbosa NHS, Vaz FF, Cordeiro LMS, Coimbra CC, Pires W, Soares DD and Wanner SP. Effects of manipulating the duration and intensity of aerobic training sessions on the physical performance of rats. PLoS One. 2017;12:e0183763. doi: 10.1371/journal.pone.0183763. [PubMed: 28841706]
43. Forouzan O, Dinges E, Runo JR, Keevil JG, Eickhoff JC, Francois C and Chesler NC. Exercise-induced changes in pulmonary artery stiffness in pulmonary hypertension. Front Physiol. 2019;10:269. doi: 10.3389/fphys.2019.00269. [PubMed: 31001123]
44. Wittstein IS, Kass DA, Pak PH, Maughan WL, Fetics B and Hare JM. Cardiac nitric oxide production due to angiotensin-converting enzyme inhibition decreases beta-adrenergic myocardial contractility in patients with dilated cardiomyopathy. Journal of the American College of Cardiology. 2001;38:429–435. doi: 10.1016/s0735-1097(01)01404-8. [PubMed: 11499734]
45. Prysyazhna O, Wolhuter K, Switzer C, Santos C, Yang X, Lynham S, Shah AM, Eaton P and Burgoyne JR. Blood pressure-lowering by the antioxidant resveratrol is counterintuitively mediated by oxidation of cGMP-dependent protein kinase. Circulation. 2019;140:126–137. doi: 10.1161/CIRCULATIONAHA.118.037398. [PubMed: 31116951]
46. Sotolongo A, Monica FZ, Kots A, Xiao H, Liu J, Seto E, Bian K and Murad F. Epigenetic regulation of soluble guanylate cyclase (sGC) beta1 in breast cancer cells. FASEB J. 2016;30:3171–3180. doi: 10.1096/fj.201600339R. [PubMed: 27279362]
47. Stepien EL, Durak-Kozica M, Kaminska A, Targosz-Korecka M, Libera M, Tylko G, Opalinska A, Kapusta M, Solnica B, Georgescu A, Costa MC, Czyzewska-Buczynska A, Witkiewicz W, Malecki MT and Enguita FJ. Circulating ectosomes: Determination of angiogenic microRNAs in type 2 diabetes. Theranostics. 2018;8:3874–3890. doi: 10.7150/thno.23334. [PubMed: 30083267]
48. Lourenco AP, Leite-Moreira AF, Balligand JL, Bauersachs J, Dawson D, de Boer RA, de Windt LJ, Falcao-Pires I, Fontes-Carvalho R, Franz S, Giacca M, Hilfiker-Kleiner D, Hirsch E, Maack C, Mayr M, Pieske B, Thum T, Tocchetti CG, Brutsaert DL and Heymans S. An integrative translational approach to study heart failure with preserved ejection fraction: a position paper from the Working Group on Myocardial Function of the European Society of Cardiology. Eur J Heart Fail. 2018;20:216–227. doi: 10.1002/ejhf.1059. [PubMed: 29148148]

49. Lu YH, Dallner OS, Birsoy K, Fayzikhodjaeva G and Friedman JM. Nuclear Factor-Y is an adipogenic factor that regulates leptin gene expression. Mol Metab. 2015;4:392–405. doi: 10.1016/j.molmet.2015.02.002. [PubMed: 25973387]
50. Nassif ME, Qintar M, Windsor SL, Jermyn R, Shavelle DM, Tang F, Lamba S, Bhatt K, Brush J, Civitello A, Gordon R, Jonsson O, Lampert B, Pelzel J and Kosiborod MN. Empagliflozin Effects on Pulmonary Artery Pressure in Patients With Heart Failure: Results From the EMBRACE-HF Trial. Circulation. 2021;143:1673–1686. doi: 10.1161/CIRCULATIONAHA.120.052503. [PubMed: 33550815]
51. Steven S, Oelze M, Hanf A, Kroller-Schon S, Kashani F, Roohani S, Welschof P, Kopp M, Godtel-Armbrust U, Xia N, Li H, Schulz E, Lackner KJ, Wojnowski L, Bottari SP, Wenzel P, Mayoux E, Munzel T and Daiber A. The SGLT2 inhibitor empagliflozin improves the primary diabetic complications in ZDF rats. Redox Biol. 2017;13:370–385. doi: 10.1016/j.redox.2017.06.009. [PubMed: 28667906]
52. Rodrigues B, Figueroa DM, Mostarda CT, Heeren MV, Irigoyen MC and De Angelis K. Maximal exercise test is a useful method for physical capacity and oxygen consumption determination in streptozotocin-diabetic rats. Cardiovasc Diabetol. 2007;6:38. doi: 10.1186/1475-2840-6-38. [PubMed: 18078520]
53. Feng J, Fitz Y, Li Y, Fernandez M, Cortes Puch I, Wang D, Pazniokas S, Bucher B, Cui X and Solomon SB. Catheterization of the carotid artery and jugular vein to perform hemodynamic measures, infusions and blood sampling in a conscious rat model. J Vis Exp. 2015. doi: 10.3791/51881.
54. Kovalski V, Prestes AP, Oliveira JG, Alves GF, Colarites DF, Mattos JE, Sordi R, Vellosa JC and Fernandes D. Protective role of cGMP in early sepsis. Eur J Pharmacol. 2017;807:174–181. doi: 10.1016/j.ejphar.2017.05.012. [PubMed: 28483456]
55. Ma Z, Mao L and Rajagopal S. Hemodynamic Characterization of Rodent Models of Pulmonary Arterial Hypertension. J Vis Exp. 2016;110:53335. doi: 10.3791/53335.
56. Kikuchi N, Satoh K, Kurosawa R, Yaoita N, Elias-Al-Mamun M, Siddique MAH, Omura J, Satoh T, Nogi M, Sunamura S, Miyata S, Saito Y, Hoshikawa Y, Okada Y and Shimokawa H. Selenoprotein P promotes the development of pulmonary arterial hypertension: Possible novel therapeutic target. Circulation. 2018;138:600–623. doi: 10.1161/CIRCULATIONAHA.117.033113. [PubMed: 29636330]
57. Umar S, Iorga A, Matori H, Nadadur RD, Li J, Maltese F, van der Laarse A and Eghbali M. Estrogen rescues preexisting severe pulmonary hypertension in rats. Am J Respir Crit Care Med. 2011;184:715–723. doi: 10.1164/rccm.201101-0078OC. [PubMed: 21700911]
58. Matyas C, Kovacs A, Nemeth BT, Olah A, Braun S, Tokodi M, Barta BA, Benke K, Ruppert M, Lakatos BK, Merkely B and Radovits T. Comparison of speckle-tracking echocardiography with invasive hemodynamics for the detection of characteristic cardiac dysfunction in type-1 and type-2 diabetic rat models. Cardiovasc Diabetol. 2018;17:13. doi: 10.1186/s12933-017-0645-0. [PubMed: 29338775]
59. Hadri L, Kratlian RG, Benard L, Maron BA, Dorfmuller P, Ladage D, Guignabert C, Ishikawa K, Aguero J, Ibanez B, Turnbull IC, Kohlbrenner E, Liang L, Zsebo K, Humbert M, Hulot JS, Kawase Y, Hajjar RJ and Leopold JA. Therapeutic efficacy of AAV1.SERCA2a in monocrotaline-induced pulmonary arterial hypertension. Circulation. 2013;128:512–523. doi: 10.1161/CIRCULATIONAHA.113.001585. [PubMed: 23804254]
60. Dahl JA and Collas P. A rapid micro chromatin immunoprecipitation assay (microChIP). Nat Protoc. 2008;3:1032–1045. doi: 10.1038/nprot.2008.68. [PubMed: 18536650]
61. Ray JC, Burger C, Mergo P, Safford R, Blackshear J, Austin C, Fairweather D, Heckman MG, Zeiger T, Dubin M and Shapiro B. Pulmonary arterial stiffness assessed by cardiovascular magnetic resonance imaging is a predictor of mild pulmonary arterial hypertension. Int J Cardiovasc Imaging. 2019;35:1881–1892. doi: 10.1007/s10554-018-1397-y. [PubMed: 29934885]
62. Plante E, Lachance D, Drolet MC, Roussel E, Couet J and Arsenault M. Dobutamine stress echocardiography in healthy adult male rats. Cardiovasc Ultrasound. 2005;3:34. doi: 10.1186/1476-7120-3-34. [PubMed: 16250913]

63. Peng G, Wang J, Lu W and Ran P. Isolation and primary culture of rat distal pulmonary venous smooth muscle cells. Hypertens Res. 2010;33:308–313. doi: 10.1038/hr.2009.234. [PubMed: 20111041]

64. Arner E, Mejhert N, Kulyte A, Balwierz PJ, Pachkov M, Cormont M, Lorente-Cebrián S, Ehrlund A, Laurencikiene J, Hedén P, Dahlman-Wright K, Tanti J-F, Hayashizaki Y, Rydén M, Dahlman I, Nimwegen Ev, Daub CO and Arner P Adipose Tissue MicroRNAs as Regulators of CCL2 Production in Human Obesity. Diabetes. 2012;61:1986–1993. doi: 10.2337/db11-1508/-/DC1. [PubMed: 22688341]

65. Morganti C, Bonora M, Ito K and Ito K. Electron transport chain complex II sustains high mitochondrial membrane potential in hematopoietic stem and progenitor cells. Stem Cell Res. 2019;40:101573. doi: 10.1016/j.scr.2019.101573. [PubMed: 31539857]

66. Radziwon-Balicka A, Degn M, Johansson SE, Warfvinge K and Edvinsson L. A novel multicolor flow-cytometry application for quantitative detection of receptors on vascular smooth muscle cells. PLoS One. 2017;12:e0186504. doi: 10.1371/journal.pone.0186504. [PubMed: 29084284]

67. Kamga Pride C, Mo L, Quesnelle K, Dagda RK, Murillo D, Geary L, Corey C, Portella R, Zharikov S, St Croix C, Maniar S, Chu CT, Khoo NK and Shiva S. Nitrite activates protein kinase A in normoxia to mediate mitochondrial fusion and tolerance to ischaemia/reperfusion. Cardiovasc Res. 2014;101:57–68. doi: 10.1093/cvr/cvt224. [PubMed: 24081164]

68. Yamazaki T, Souquere S, Chujo T, Kobelke S, Chong YS, Fox AH, Bond CS, Nakagawa S, Pierron G and Hirose T. Functional Domains of NEAT1 Architectural lncRNA Induce Paraspeckle Assembly through Phase Separation. Mol Cell. 2018;70:1038-1053 e1037. doi: 10.1016/j.molcel.2018.05.019. [PubMed: 29932899]

69. Tani H and Akimitsu N. Genome-wide technology for determining RNA stability in mammalian cells: historical perspective and recent advantages based on modified nucleotide labeling. RNA Biol. 2012;9:1233–1238. doi: 10.4161/rna.22036. [PubMed: 23034600]

Clinical Perspective

What is new?

- This study describes new rat models of EIPH in HFpEF and CpcPH, modeling human conditions associated with high morbidity and mortality.
- The exercise-induced alterations in the models are caused by PA functional impairment mediated by the transcriptional down-regulation of sGCβ1 in PAVSMCs.
- A novel regulatory pathway causes pulmonary hypertension mediated by mitochondrial ROS-induced expression of miR-193b, which degrades the messenger RNA coding NFYA, a critical transcription factor that controls sGCβ1 expression in PAVSMCs.
- *In vivo*, forced expression of NFYA using rAAV6 gene delivery, or upstream inhibition of the metabolic syndrome with SGLT2 inhibitor, improves exercise-PH in CpcPH models, accompanied by improvements in NYFA-sGC-cGMP signaling.

What are the clinical implications?

- New models of exercise-induced PH in CpcPH and HFpEF contribute to further understanding of pathophysiology and reveals new targets for therapy.
- These results uncover a molecular explanation for the unsolved clinical associations linking metabolic syndrome with EIPH in patients with CpcPH and HFpEF, such as enhanced mitochondrially-derived ROS and depletion of NFYA-sGCβ1 in the pulmonary arterial vasculature.
- This study suggests new therapeutic approaches targeting upstream mechanisms of EIPH in HFpEF using overexpression of NFYA or SGLT2 inhibitors.

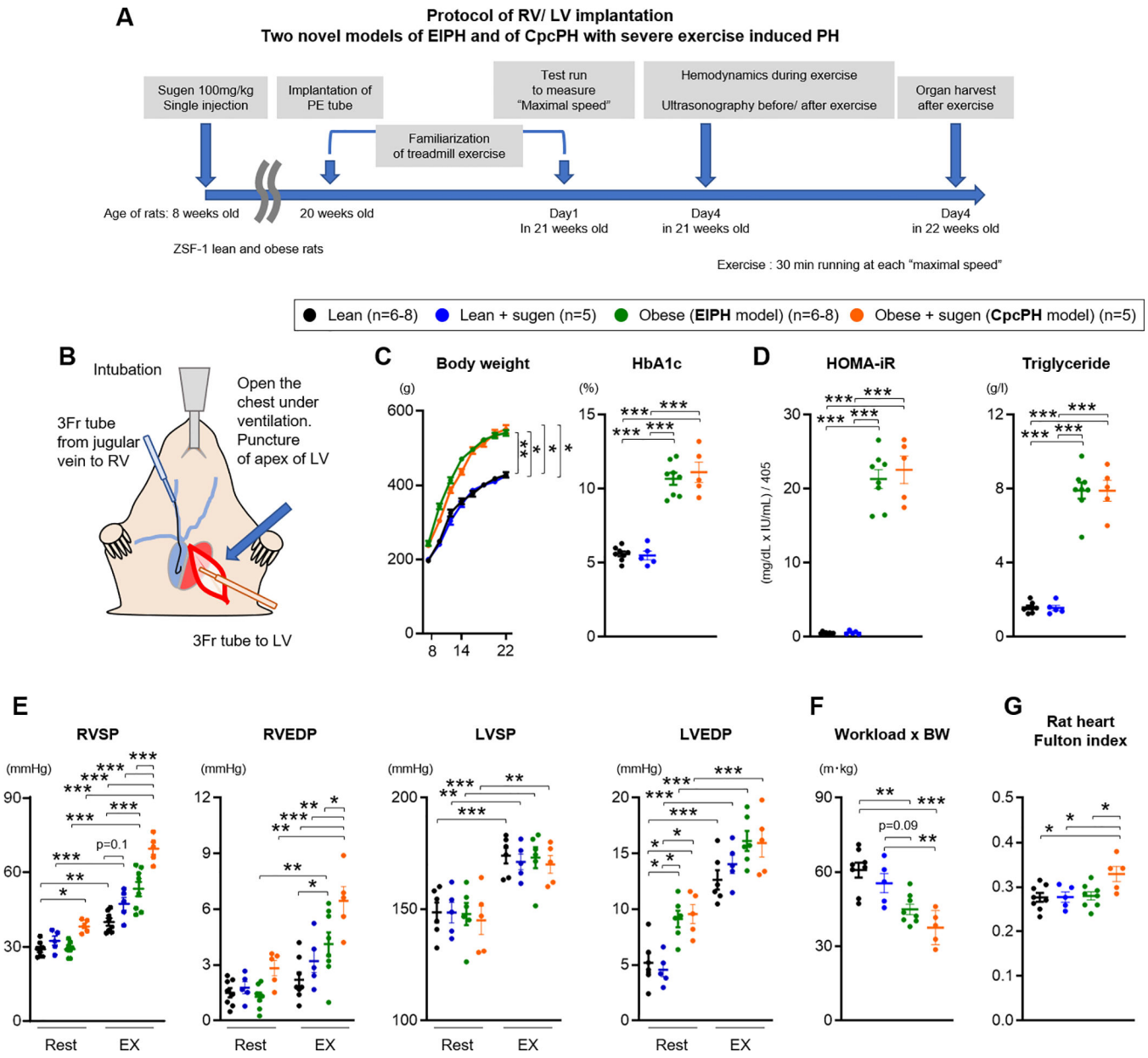

Figure 1. Novel HFpEF rat and CpcPH model of Exercise Induced Pulmonary Hypertension

(**A**) Experimental timeline for lean, lean treated with sugen, obese (EIPH model), and obese treated with sugen rats (CpcPH model). (**B**) Representative image of implantation of polyethylene (PE) tube in right (RV) and left ventricle (LV). (**C-D**) At 22 weeks old of age, Body weight, HbA1c level, HOMA-iR and Tryiglyceride were measured (lean n=8, lean+sugen n=5, obese n=8, obese+sugen n=5). (**E**) Right ventricular systolic and end-diastolic pressure (RVSP and RVEDP), left ventricular systolic and end-diastolic pressure (LVSP and LVEDP) were measured at rest and during exercise (lean n=6–8, lean+sugen n=5, obese n=6–8, obese+sugen n=5). (**F**) Workload were calculated with the distance of test run and body weight (BW) (lean n=8, lean+sugen n=5, obese n=8, obese+sugen n=5). (**G**) Fulton index was measured as weight of RV/weight of LV + septum in lean

(n=8), lean+sugen (n=5), obese (n=8), and obese+sugen rats (n=5). Results are expressed as mean±SEM. *P<0.05, **P<0.01, ***P<0.001. Comparisons of parameters were performed with 2-tailed Student's t-test, Welch's t-test, one-way ANOVA, repeated measure two-way ANOVA or mixed-effects model analysis followed by Tukey's honestly significant difference (HSD) test for multiple comparisons.

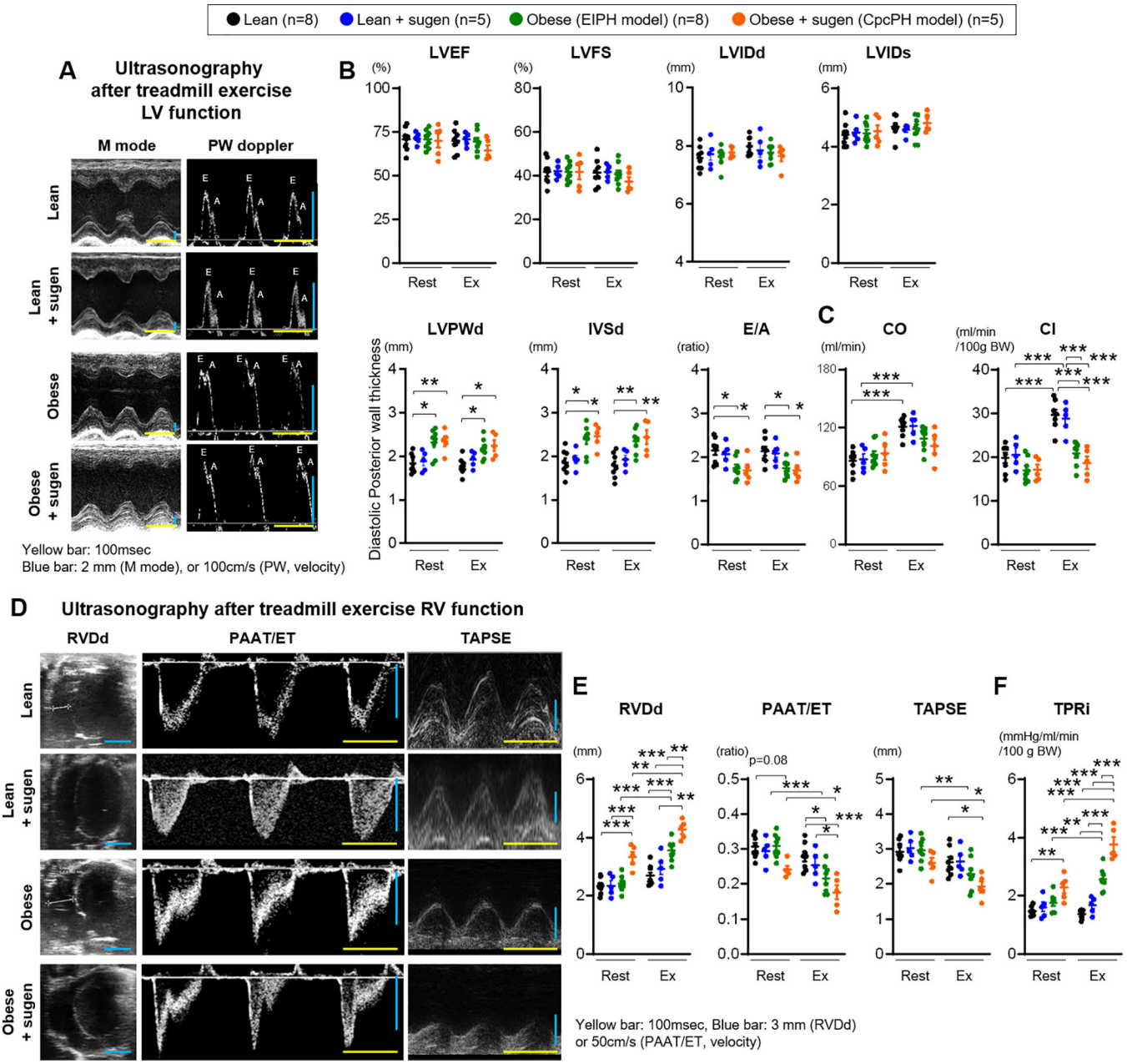

Figure 2. Right ventricular dysfunction after exercise in ZSF-1 obese and obese+sugen models.

(**A**) Representative images from M mode and pulse-wave (PW) doppler mode ultrasonography. Yellow scale bar, 100 msec. Blue scale bar, 2 mm (M mode), or 100 cm/s (PW mode). (**B-C**) Left ventricular Ejection fraction (LVEF), Fraction shortening (LVFS), Internal diastolic or systolic diameter (LVIDd or LVIDs), end-diastolic posterior wall (LVPWd), end-diastolic interventricular septal wall thickness (IVSd), E wave/A wave ratio (E/A), cardiac output (CO), and cardiac index (CI) were measured at rest and during exercise. (**D**) Representative images of M mode and PW doppler mode ultrasonography used to calculate right ventricular end-diastolic diameter (RVDd), pulmonary artery acceleration time (PAAT) per ejection time (ET), and tricuspid annular plane systolic excursion (TAPSE).

Yellow scale bar, 100 msec. Blue scale bar, 3 mm (RVDd or TAPSE), or 100 cm/s (PAAT/ET). (**E-F**) RVDd, PAAT/ET, TAPSE, and TPRi were measured at rest and after exercise. Rats per group; lean n=8, lean+sugen n=5, obese n=8, obese+sugen n=5. Results are expressed as mean±SEM. *P<0.05, **P<0.01, ***P<0.001. Statistical analyses were performed as described in Figure 1 legend.

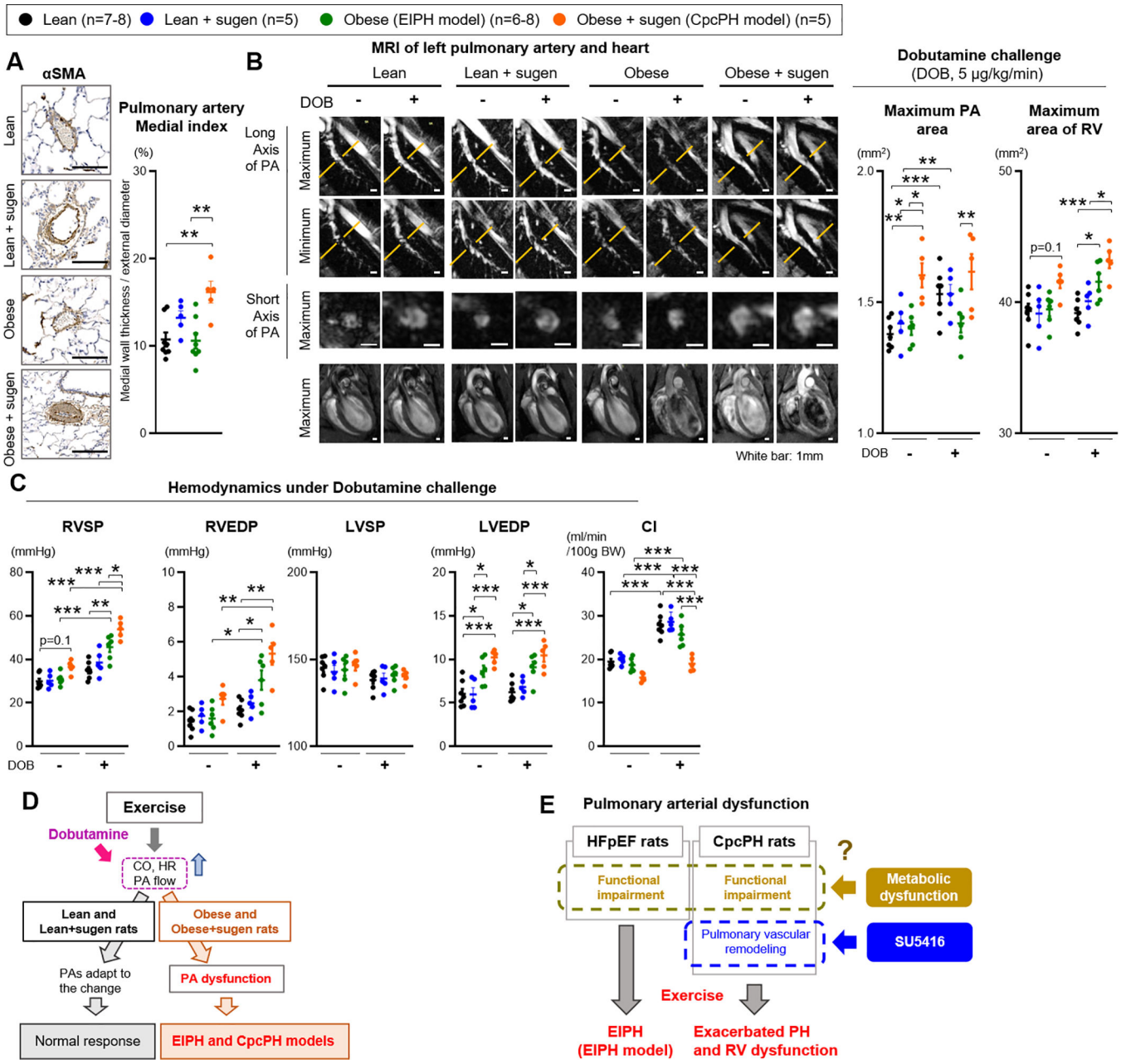

Figure 3. Pulmonary artery dysfunction contributes to the pathophysiology in EIPH and in CpcPH during exercise

(**A**) Representative immunostaining for α-smooth muscle actin (αSMA) of the pulmonary arteries in lean, obese, obese+sugen rats. Scale bars, 100 μm. Medial index (%) of distal pulmonary arteries with a diameter of 20–100 μm was calculated as described in Methods in lean (n=8), lean+sugen (n=5), obese (n=8), and obese+sugen rats (n=5). (**B**) Representative images of MRI of left pulmonary artery and heart at rest and during dobutamine (5μg/kg/min) challenge in lean, lean+sugen, obese, and obese+sugen rats. White bars indicate 1 mm. Quantification of area of left pulmonary artery at second branch and area of right ventricular in lean (n=6–7), lean+sugen (n=5), obese (n=6), and obese+sugen rats (n=5).

(**C**) Hemodynamics (RVSP, RVEDP, LVSP, and LVEDP) and cardiac index (CI) during dobutamine challenge in lean (n=6–7), lean+sugen (n=5), obese (n=6), and obese+sugen rats (n=5). (**D**-**E**) Schematic representation of the mechanisms underlying pulmonary artery and right ventricular dysfunction in EIPH in obese and obese+sugen rats. Results are expressed as mean±SEM. **P*<0.05, ***P*<0.01, ****P*<0.001. Statistical analyses were performed as described in Figure 1 legend.

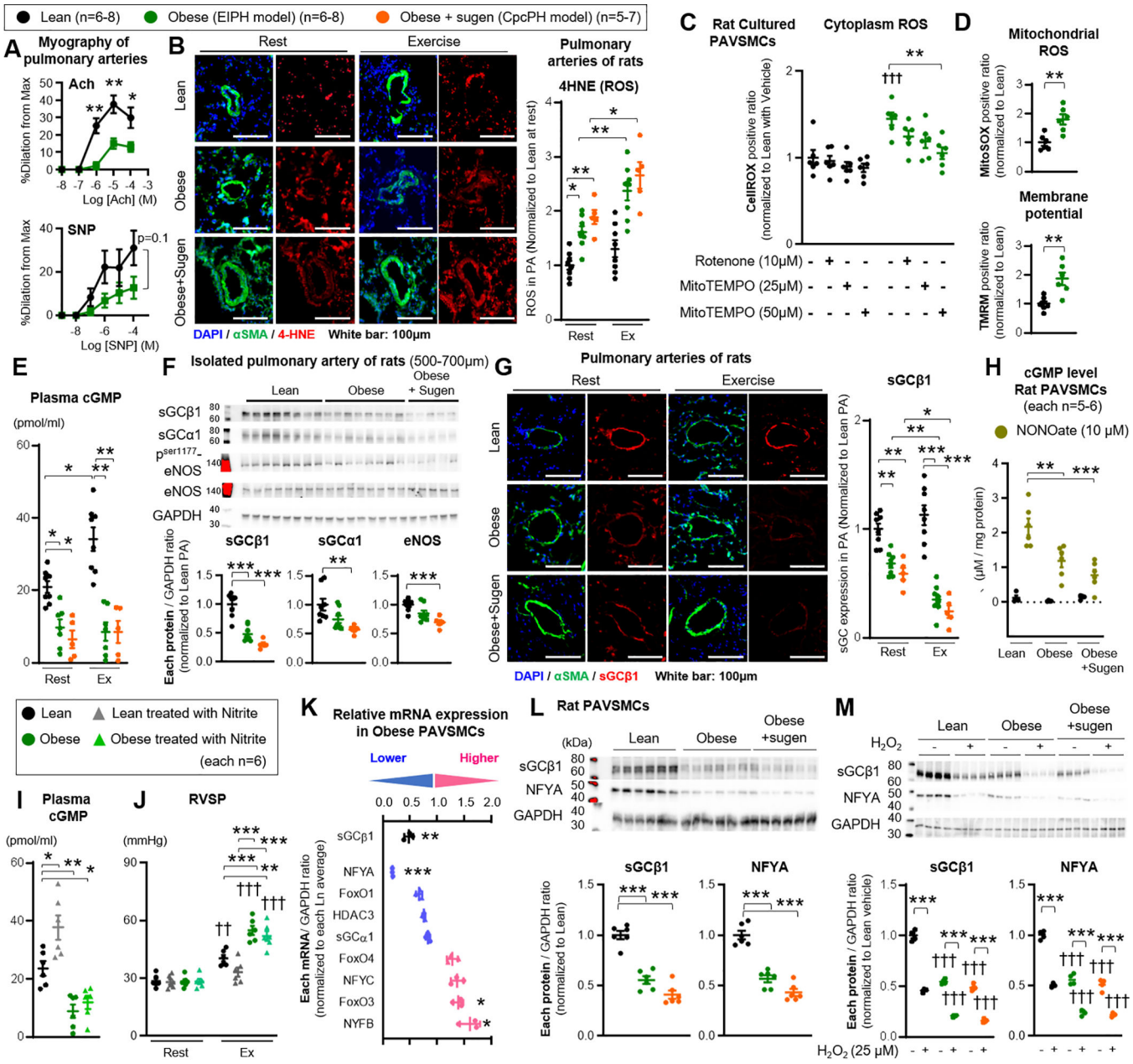

Figure 4. Increased mitochondrial derived ROS and decreased sGC enzyme expression and activity in PAVSMCs

(**A**) Myographic studies on isolated pulmonary arteries of lean and obese rats with acetylcholine (Ach) or sodium nitroprusside (SNP) (each n=6). (**B**) Representative immunofluorescence images and quantification of 4HNE of distal pulmonary arteries. lean n=8, obese n=8, and obese+sugen (n=5) at rest or after treadmill exercise. (**C**) Quantification of intra-cellular ROS (CellROX fluorescence) in cultured PAVSMCs from lean and obese rats, in which Rotenone (10μM) and MitoTEMPO (25 or 50μM) were added 10 minutes before analysis (each n=6). (**D**) Quantification of mitochondrial ROS (MitoSOX fluorescence) or membrane potential (TMRM fluorescence) in cultured PAVSMCs from lean and obese rats (each n=6). (**E**) Quantification of cGMP of plasma level in lean (n=7),

obese (n=6), and obese+sugen rats (n=5). (**F**) Representative Western blot and quantification of sGCβ1, sGCα1, phosphorylation ser1177 eNOS, total eNOS and GAPDH in isolated pulmonary arteries of lean (diameter of PAs: 500–700μm) (n=8), obese (n=8), and obese+sugen rats (n=5). (**G**) Representative immunofluorescence image and quantification of sGCβ1 of distal pulmonary arteries. lean n=8, obese n=8, and obese+sugen (n=5) at rest or after treadmill exercise. (**H**) cGMP level in PAVSMCs of lean, obese, obese+sugen rats treated with NO donor DETA NONOate (10μM, 24 hours) (each n=6). (**I-J**) Lean and obese rats were treated with Nitrites via drinking water (100mg/L) or vehicle for 1-week. Quantification of cGMP of plasma level (each n=6). Right ventricular systolic pressure (RVSP) was measured at rest and during exercise (each n=6). (**K**) Quantification of relative mRNA expression of sGCβ1, sGCα1, NFYA, NFYB, NFYC, FoxO1, 3 and 4, and HDAC3 in cultured PAVSMCs from obese rats compared to lean rats (n=3, each) (*P<0.05, **P<0.01, ***P<0.001 vs Ln). (**L**) Representative Western blot and quantification of sGCβ1, NFYA, and GAPDH in cytoplasm in lean, obese and obese+sugen PAVSMCs (n=6, each). (**M**) Representative Western blot and quantification of sGCβ1, NFYA, and GAPDH in rat PAVSMCs treated with hydrogen peroxidase (H_2O_2, 25μM, 24 hours) (n=3, each). Results are expressed as mean±SEM. *P<0.05, **P<0.01, ***P<0.001. †† P<0.01, ††† P<0.001 vs same group at condition. Statistical analyses were performed as described in Figure 1 legend.

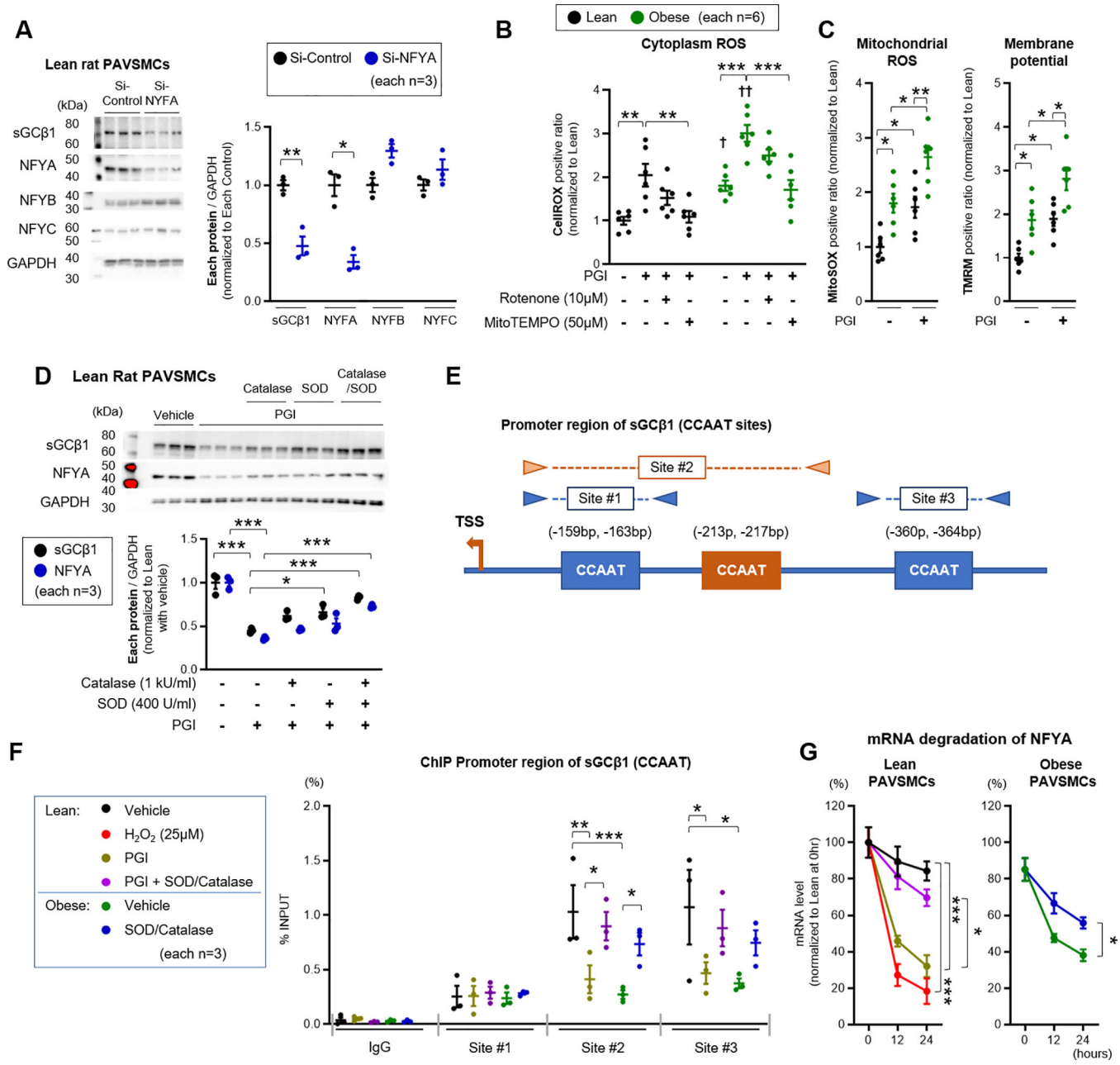

Figure 5. Transcription factor NFYA controls sGC expression in PAVSMCs and is down regulated by metabolic stress and ROS

(**A**) Representative Western blot and quantification of sGCβ1, NFYA, NFYB, NFYC, and GAPDH in PAVSMCs treated with Si-Control or Si-NYFA (each n=3). Each plot represents the PAVSMCs sample cultured from one individual rat. (**B-C**) Quantification of intra-cellular ROS (CellROX fluorescence), mitochondrial ROS (MitoSOX fluorescence), and membrane potential (TMRM fluorescence) in rat PAVSMCs treated with Palmitate acid (P, 0.2 mM) and Glucose (G, 25 mM), Insulin (I, 120 nM) stimulation for 24 hours, in which Rotenone (10μM) and MitoTEMPO (50μM) were added 10 minutes before analysis (each n=6). (**D**) Representative Western blot and quantification of sGCβ1, NFYA

and GAPDH in lean rat PAVSMCs treated with superoxide dismutase (SOD, 400 U/ml), Catalase (1 kU/ml) or PGI for 24 hours (n=6, each). (**E-F**) Transcription binding sites for promoter region of sGCβ1 (CCAAT sequence). Chromatin immunoprecipitation (ChIP) showing enrichment of NYFA at sGCβ1 promoter in lean and obese PAVSMCs treated with PGI, SOD or Catalase (each n=3). (**G**) RNA degradation of NFYA for 12 or 24 hours in lean and obese rat PAVSMCs treated with PGI, hydrogen peroxidase (H_2O_2, 25 μM), superoxide dismutase (SOD, 400 U/ml), or catalase (1 kU/ml) (n=3). Results are expressed as mean±SEM. **P*<0.05, ***P*<0.01, ****P*<0.001. † *P*<0.05, †† *P*<0.01 vs same group at condition. Statistical analyses were performed as described in Figure 1 legend.

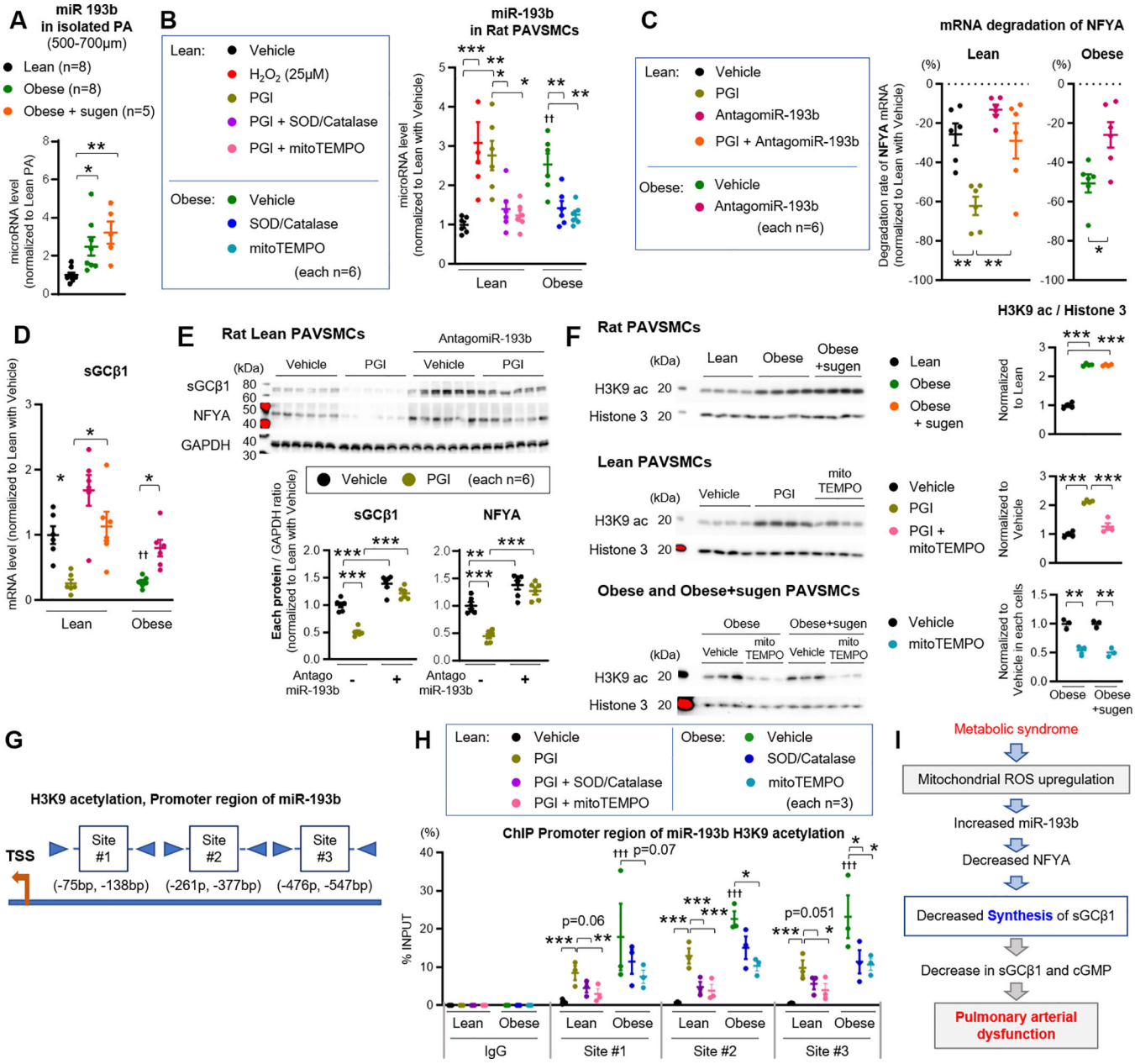

Figure 6: miR-193b promotes ROS-dependent degradation of NFYA, reducing sGC transcription

(**A**) Quantification of miR-193b expression in pulmonary arteries (diameter of PAs: 500–700μm) from lean (n=8), obese (n=8), and obese+sugen rats (n=5). (**B**) miR-193b expression in lean and obese rat PAVSMCs treated with hydrogen peroxidase (H_2O_2, 25 μM), superoxide dismutase (SOD, 400 U/ml), catalase (1 kU/ml) or mitoTEMPO (50μM) (n=6). (**C**) mRNA degradation rate of NFYA for 24 hours in lean and obese rat PAVSMCs treated with PGI or Antagomir-193b (n=6). (**D-E**) Expression of sGCβ1 mRNA and protein level in lean and obese rat PAVSMCs treated with PGI or AntagomiR-193b (n=6). (**F**) Representative Western blot and quantification of H3K9ac and Histone 3 in lean PAVSMCs treated with PGI or mitoTEMPO or obese and obese+sugen PAVSMCs treated with mitoTEMPO (n=3–4). (**G-H**) Transcription binding sites for promoter region

of miR-193b. Chromatin immunoprecipitation (ChIP) showing enrichment of H3K9ac at miR-193b promoter in lean and obese PAVSMCs treated with PGI, SOD, Catalase, or mitoTEMPO (each n=3). (**I**) Schematic representation of the molecular mechanisms underlying reactive oxygen species (ROS) and sGCβ1/NFYA/miR-193 expression, resulting in pulmonary arterial relaxation dysfunction. Results are expressed as mean±SEM. *P<0.05, **P<0.01, ***P<0.001. † P<0.05, †† P<0.01, ††† P<0.001 vs Lean PAVSMCs at same condition. Statistical analyses were performed as described in Figure 1 legend.

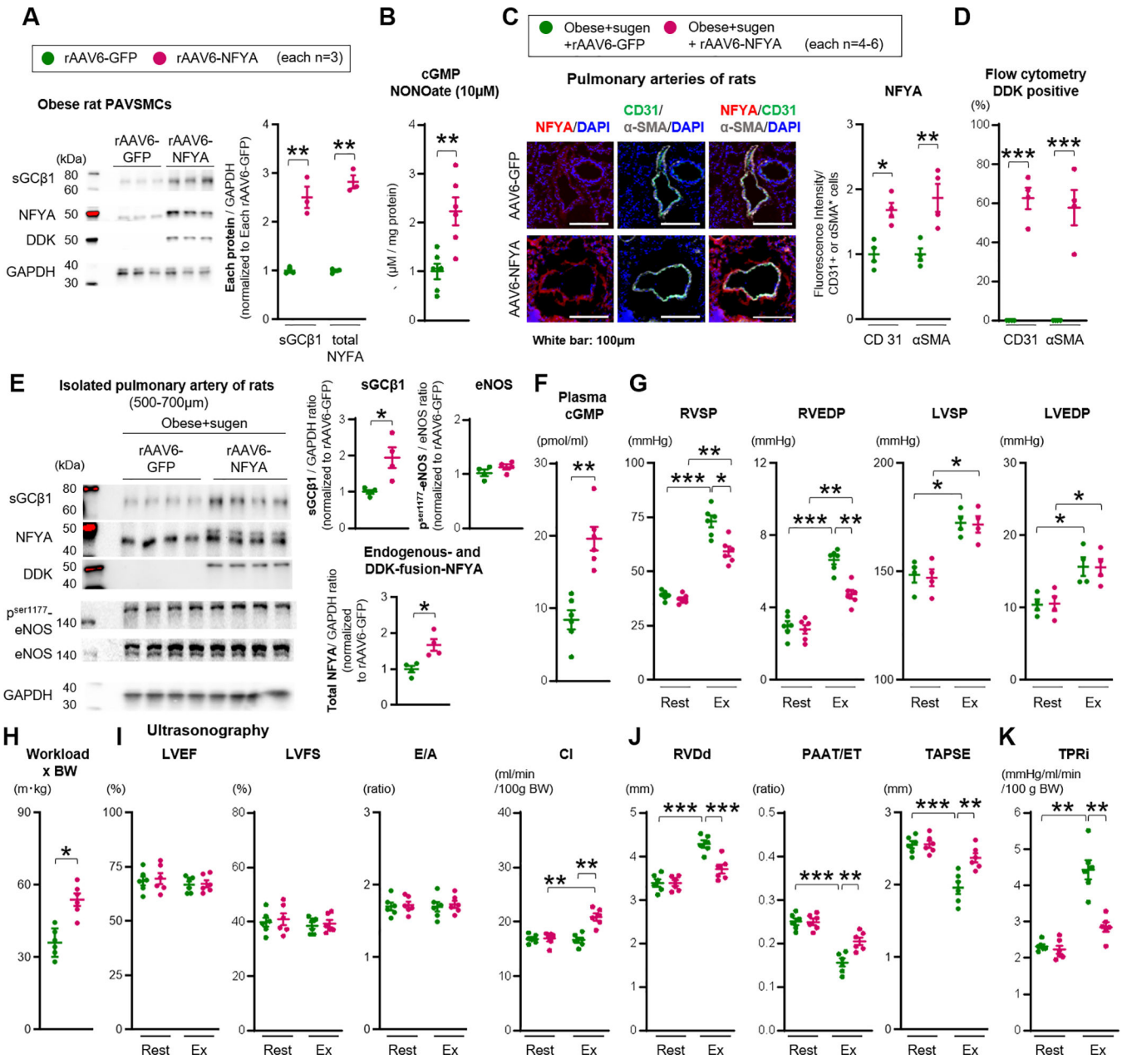

Figure 7. Forced sGC activity and NFYA expression rescue exercise induced pulmonary hypertension in CpcPH rats

(**A**) Representative Western blot and quantification of sGCβ1, total NFYA (endogenous 44kDa and DDK-fusion 50kDa), DDK, and GAPDH in PAVSMCs infected with rAAV6-GFP or rAAV6-NFYA-DDK (each n=3). Each plot represents the PAVSMCs sample cultured from one individual rat. (**B**) cGMP level in PAVSMCs of obese treated with rAAV6-NFYA-DDK or rAAV6-GFP and NO donor DETA NONOate (10μM, 24 hours) (each n=6). (**C**) Administration of rAAV6-GFP or rAAV6-NFYA-DDK to obese+sugen rats. Representative immunofluorescence images and quantification of NFYA, CD31, αSMA, and DAPI of pulmonary arteries (each n=4). (**D**) Flow cytometry showing the percent of DDK in CD31 or αSMA positive cells (each n=4). (**E**) Representative Western blot

and quantification of sGCβ1, total NFYA (endogenous 44kDa and DDK-fusion 50kDa), phosphorylation ser 177 eNOS, total eNOS and GAPDH in isolated pulmonary arteries of rats (diameter of PAs: 500–700μm) (each n=4). (**F**) Quantification of plasma levels of cGMP of the rats (each n=6). (**G-H**) Right ventricular systolic and end-diastolic pressure (RVSP and RVEDP, each n=6), left ventricular systolic and end-diastolic blood pressure (LVSP and LVEDP, each n=4), and Workload (each n=6) were measured at rest and during exercise (obese+sugen rats infected with rAAV6-GFP or rAAV6-NFYA-DDK). (**I-K**) Left ventricular Ejection fraction (LVEF), Fraction shortening (LVFS), E wave/A wave ratio (E/A), cardiac index (CI), RVDd, PAAT/ET, TAPSE, and TPRi were measured at rest and during exercise. Rats per group; obese+sugen rats infected with rAAV6-GFP or rAAV6-NFYA-DDK (each n=6). Results are expressed as mean±SEM. **P*<0.05, ***P*<0.01, ****P*<0.001. Statistical analyses were performed as described in Figure 1 legend.

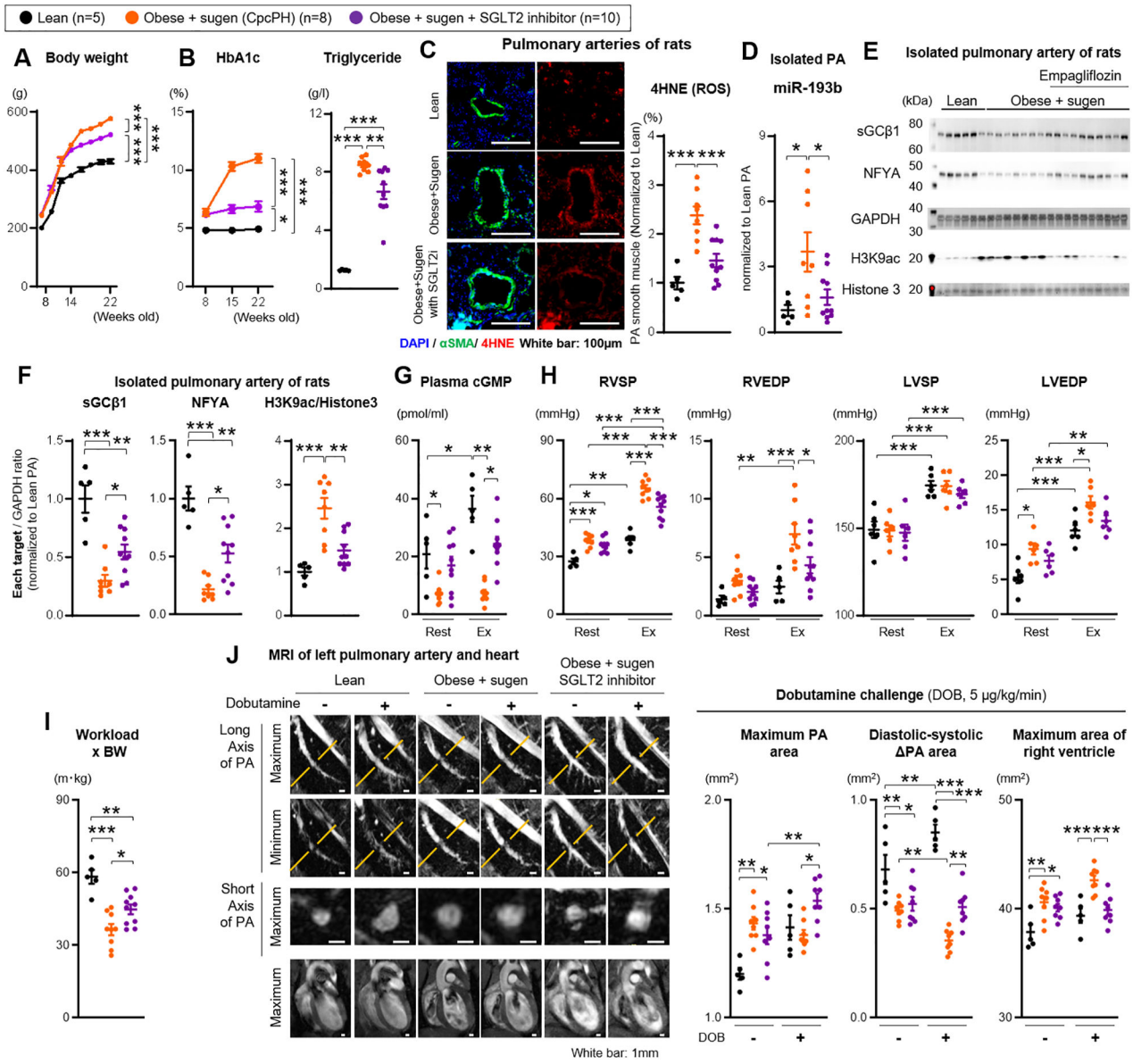

Figure 8. Upstream treatment of metabolic syndrome with SGLT2 inhibition rescues mitochondrial ROS in PAVSMCs and restores the NFYA-sGC-cGMP signaling to improve CpcPH

Treatment with SGLT2 inhibitor (Empagliflozin 10 mg/kg/day, via drinking water) in obese rats treated with sugen (Obese+sugen). (**A-B**) Body weight and HbA1c level were measured from 8 to 22 weeks old. At 22 weeks old, triglyceride plasma level was measured (lean n=5, obese+sugen n=8, obese+sugen+SGLT2 inhibitor n=10). (**C**) Representative immunofluorescence images and quantification of 4HNE (4-hydroxynonenal), αSMA and DAPI of pulmonary arteries in lean (n=5), obese+sugen (n=8), and obese+sugen treated with SGLT2 inhibitor (n=10). (**D**) Quantification of miR-193b expression in pulmonary arteries from lean (n=5), obese+sugen (n=8), and obese+sugen treated with SGLT2 inhibitor (n=10). (**E-F**) Representative Western blot and quantification of sGCβ1, NFYA, GAPDH, H3K9 ac, and Histone 3 in isolated pulmonary arteries (diameter of PAs: 500–700μm) of

lean (n=5), obese+sugen (n=8), and obese+sugen treated with SGLT2 inhibitor (n=10). (**G**) Quantification of plasma levels of cGMP in lean (n=5), obese+sugen (n=8), and obese+sugen treated with SGLT2 inhibitor (n=10). (**H**) Right ventricular systolic and end-diastolic pressure (RVSP and RVEDP), left ventricular systolic and end-diastolic blood pressure (LVSP and LVEDP) were measured at rest and during exercise (lean n=5, obese+sugen n=8, obese+sugen+SGLT2 inhibitor n=10). (**I**) Workload were calculated with the distance of test run (lean n=5, obese+sugen n=8, obese+sugen+SGLT2 inhibitor n=10). (**J**) Representative images of MRI of left pulmonary artery and heart at rest and during dobutamine (5μg/kg/min) challenge in lean, obese+sugen, and obese+sugen treated with SGLT2 inhibitor. White bars indicate 1 mm. Quantification of area of left pulmonary artery at second branch and area of RV in lean (n=5), obese+sugen (n=8), and obese+sugen treated with SGLT2 inhibitor (n=8). Results are expressed as mean±SEM. *P<0.05, **P<0.01, ***P<0.001. Statistical analyses were performed as described in Figure 1 legend.